Phyllanthus emblica Loaded Cryogels for Improved Wound Care: Characterizationand In Vitro Studies

İpek CANATAR , Sibel ÖZDAŞ * , Gözde Baydemir Pesint

Posted Date: 16 February 2024

doi: 10.20944/preprints202311.1288.v2

Keywords: *Phyllanthus emblica*; cryogel; wound dressing materials; wound healing

 doi:10.20944/preprints202311.1288.v2

Article

Phyllanthus emblica Loaded Cryogels for Improved Wound Care: Characterization and In Vitro Studies

İpek CANATAR, Sibel ÖZDAŞ * and Gözde BAYDEMİR PEŞİNT

Department of Bioengineering, Faculty of Engineering Sciences, Adana Alpaslan Türkeş Science and Technology University, Adana, Türkiye; icanatar@atu.edu.tr (İ. C.); gpesint@atu.edu.tr (G.B.P.)
* Correspondence: sozdas@atu.edu.tr; Tel: +90 4550000-2157

Abstract: Wound dressings developed by combining plant extracts with polymers have made a great progress in wound care treatment. One plant with remarkable healing properties is *Phyllanthus emblica Linn* (*P. emblica*), which has been described as having potent antioxidant, antimicrobial and anti-inflammatory properties. The aim of this study was to evaluate the biocompatibility of *P. emblica* loaded polyvinylalcohol/gelatin based cryogels (PVA/Gel/*P.emblica*) through cytotoxicity and proliferation tests in HaCaT cells and examine their potential in wound dressing applications. Accordingly, PVA/Gel/*P.emblica* cryogels were successfully synthesized and characterization studies and in vitro cell culture studies were performed. The swelling tests and BET analysis results showed that swelling and surface area properties of cryogels increased with increasing *P. emblica* amounts. Morphological results displayed that the cryogels had a dense, interconnected pore morphology and a macroporous structure. 3-(4,5-dimethylthiazol-2-yl)-2,5-diphenyltetrazolium bromide (MTT), trypan blue exclusion and live-dead assay results revealed that *P. emblica* enhanced cell proliferation, increased cell number and improved cell viability. Based on the scanning electron microscope (SEM), immunofluorescence and giemsa staining images, it was observed that *P. emblica* promoted cell attachment, proliferation and penetration. These findings confirm that PVA/Gel/*P.emblica* cryogels are suitable for use as wound dressing materials and can be developed with further studies.

Keywords: Wound healing; *Phyllanthus emblica*; cryogel; wound dressing materials

1. Introduction

The skin is the first line of defense of the human body, which surrounds the body and acts as a barrier against external factors [1]. Infections cause illness and death in millions of people worldwide due to the lack of effective wound care [2]. The primary purpose of wound care is to protect the wounds from further damage caused by the loss of moisture, the presence of microorganisms and external factors [3]. Throughout history, wound care and healing have been supported by various types of materials and structures to maintain skin integrity [4]. Considering the complex nature of the wound healing process, it is of great importance to choose the appropriate treatment method [4]. Currently, wound dressings are mainly used to protect wounds from infection and to facilitate the regeneration and maintenance of dermal and epidermal tissues during the wound healing process [5,6]. Wound dressings should provide a barrier to the wound area against external factors, keep the wound area moist, and permit gas exchange to ensure optimal healing. In addition to these properties, they should be non-toxic, non-adherent, non-allergenic, non-inflammable, comfortable, biocompatible and biodegradable [7].

Owing to their distinctive properties, such as adequate flexibility, hydrophilicity, superabsorbancy, and softness, hydrogels have become appealing candidates for use as wound dressings [8]. However, a major drawback of hydrogels is their low mechanical stability at swollen state which complicates their usage [9,10]. In contrast, cryogels which are macroporous structures offering superior physical properties compared to hydrogels are highly desirable for various

 doi:10.20944/preprints202311.1288.v2

biomedical applications, especially for wound dressings [11,12]. Cryogels are fabricated via cryogelation process at subzero temperatures which allows the formation of the large interconnected macroporous structure of the cryogel (Figure 1) [13]. This macroporous structure enables mass fluid transfer and high surface area to volume ratio for cell growth or drug loading [14]. Cryogels exhibit advanced swelling and mechanical properties as well as interconnected porous structures [10].

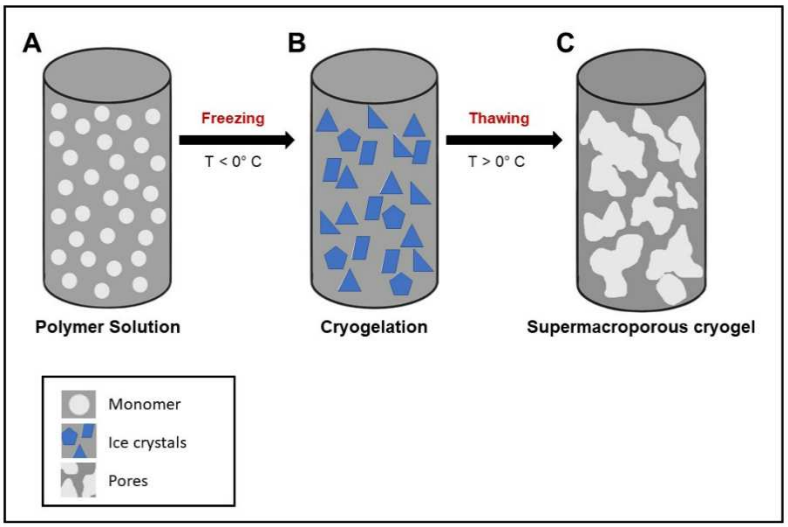

Figure 1. Schematic representation of the synthesis of cryogel. A) Solution of monomer and an aqueous solvent; B) cryogelation achieved after sub-zero incubation and ice crystal formation. C) formation of mature super-macroporous cryogel.

Cryogels can be composed of natural and synthetic polymers as well as their combinations [15]. Synthetic polymers that are used for the synthesis of cryogel wound dressings are poly(vinyl alcohol) (PVA), polyglycolic acid, poly-l-lactic acid (PLLA), poly(lactic acid) (PLA) and poly(ethylene glycol) (PEG). Natural polymers such as alginate, gelatin (Gel), collagen, silk fibroin (SF), chitosan and hyaluronic acid (HA), are also frequently used [16,17]. These polymers can be combined with materials such as different drugs and plant extracts to possess antioxidant and antimicrobial properties [17,18].

Plant-based therapies have been a source of medical treatment since ancient times. Nowadays, many different medicinal plants and their extracts are being studied and utilized to treat wounds because of their potential reparative and therapeutic effects on wounds [19]. The medicinal value of plants depends on the presence of phytochemical components such as flavonoids, tannins, alkaloids and phenolic compounds. The wound healing process is supported and accelerated by bioactive substances found in plants. These herbal extracts are added to wound dressing materials to aid wound shrinkage, epithelialization and vascularization, thereby accelerating the wound healing process [20]. Recent advances in wound dressings developed with the combination of plants with polymers enable great progress in wound care treatment [21].

Phyllanthus emblica Linn *(P. emblica; Emblica officinalis* Gaertn) is a medicinal plant from the Phyllanthaceae family, also known as the Indian gooseberry or amla. It is distributed throughout tropical and subtropical regions of India, Indonesia, Uzbekistan, Pakistan, Southeast Asia, China, Srilanka and Malaysia [22,23]. In accordance with the belief in traditional Indian mythology, *P. emblica* is considered as the first tree to be created in the universe [24]. *P. emblica* has been used in medicinal systems including Ayurveda for centuries due to its unique restorative and rejuvenating potential. Moreover, it is considered as "the King of Rasyana" in Ayurveda because of its amazing rejunavation and reconstructive abilities. *P. emblica* has been used for the treatment of various diseases including asthma, cough, diabetes, diarrhea, cancer, hepatic disorders, peptic ulcer, inflammation, jaundice and heart diseases [25,26]. Previous studies revealed that *P. emblica* extracts possess strong antioxidant, anti-microbial and anti-inflammatory properties [27]. Antioxidants are

 doi:10.20944/preprints202311.1288.v2

thought to aid tissue repair during wound healing by helping to defend against oxidative stress and inflammation [22]. The activity of *P. emblica* extract on wound healing has also been investigated in various studies, and in vitro studies have shown that *P. emblica* exhibits significant wound healing activity through the proliferation and mobilization of fibroblasts and keratinocytes [28–30]. Documented that *P. emblica* has a high antioxidant capacity and improved endothelial wound healing at low concentrations. However, it was observed to have an adverse effect on wound healing at high concentrations [30]. The wound healing model of *P. emblica* in the Wistar albino rat was investigated. This study demonstrated 95% regeneration of the dermis and epidermis in *P. emblica* treated rats over a 16-day period. Treated rats showed higher amounts of type 1 collagen along with better maturation and crosslinking, thus verifying the role of *P. emblica* in wound healing [31]. In this present work, *P. emblica* was loaded into PVA and Gel based cryogels, and characterization and in vitro studies was performed to evaluate the possibility of synthesized cryogels as wound dressing materials. The aim of this study was to assess the wound healing, cytotoxicity, migratory activities of *P. emblica* loaded wound dressing materials in HaCaT cells.

2. Materials and Methods

2.1. Preparation of P. emblica Loaded Wound Dressing Materials

P. emblica in powder form was provided by Sabinsa Corporation, USA. PVA powder (99% hydrolyzed, Sigma-Aldrich, USA) was dissolved in ultrapure water (10% w/v) under slow stirring at 80°C. Gel (bovine skin, Sigma-Aldrich, USA) solution was prepared in ultrapure water (3% w/v) at 40 °C in a water bath. After that, PVA and Gel were mixed at a ratio of 1:2 (v/v). *P. emblica* powder was dissolved in 5% DMSO (v/v) solution and then it was filtered through sterile Millex® Syringe Filters (0,22 μm). Different concentrations of *P. emblica* (0.5%, 1%, 1.5% and 2%) were added into the polymeric solution under magnetic stirring. Finally, glutaraldehyde (2% weight of total polymer amount) (Merck, Germany) was added as a crosslinker to the polymer mixture. After adding glutaraldehyde, the polymer mixture was mixed at low speed for 15 seconds and then poured into a 24 well plate. The whole mixing process was completed within 5 minutes. For comparison, cryogel without *P. emblica* was also synthesized according to the same protocol. Finally, the mixture was poured into 24 well plates and cooled in the freezer at -16 °C for 12 hours. After the polymerization process, the cryogels were thawed at room temperature and washed several times with distilled water to remove the unreacted polymers and crosslinkers.

2.2. Swelling Tests

Cryogels were dried by lyophilizer (BK-FD10, Biobase) at -55°C for 2 hours and then dry samples (m_d) were weighed. The dried cryogels were immersed in ultrapure water. The swollen cryogels were weighed (m_{sw}) at regular time intervals until equilibrium was achieved. Excess water was wiped off from the swollen cryogels before weighing them. The swelling ratio (SR %) was determined using the formula

$$SR\ (\%) = (m_{sw}-m_d)/m_d \times 100\% \quad (1)$$

where m_d are the weight of the dry cryogel before swelling, m_{sw} is the weight of the swollen cryogel.

For the polymerization yield of cryogels, the total amount of components added to the polymer solution was recorded (m_t). The polymerization yield was calculated according to Equation 2.

$$\text{Polymerization yield } (\%) = (m_d / m_t) \times 100\% \quad (2)$$

The swollen and squeezed cryogel weights were recorded to determine the macroporosity of cryogels. In this regard, cryogels were immersed in ultrapure water until swelling. The swollen cryogels (m_{sw}) was weighted. After the swelling process was completed, swollen cryogels were squeezed and weighed (m_{sq}) [32,33]. The macroporosity of cryogels were calculated according to Equation 3.

$$\text{Macroporosity } (\%) = (m_{sw} - m_{sq})/m_{sw} \times 100\% \quad (3)$$

The same calculations were applied for all cryogels. The experiments were repeated three times and mean values were calculated.

 doi:10.20944/preprints202311.1288.v2

2.3. BET Analysis

The specific surface area is one of the most important properties of porous materials to be detected. BET analysis was carried out to investigate the surface areas of the prepared PVA/Gel and PVA/Gel/*P.emblica* cryogels. BET analysis enables the determination of the surface area of the material through the nitrogens' strong interaction with solids and its availability of high purity. Nitrogen adsorption of the vacuum-dried samples was carried out at 77 K (196°C). Finally, the specific surface area of the sample was calculated with utilization of the amount of adsorbed nitrogen, as a unit of m^2/g.

2.4. Morphology Analysis

The surface morphology and bulk structures of cryogels were assessed with a Scanning Electron Microscope (SEM) (Quanta FEG 650, Thermofisher, Massachusetts, USA). SEM is an effective imaging method utilized to display the morphology of cryogels [34]. The cryogels were frozen at -20°C and frozen cryogels were dried at -55°C via lyophilizer. After that, they were coated with gold-palladium (2:3) and viewed under an SEM. Image J software was employed to determine the pore size and distribution of these pores of the cryogels. In addition, a camera optical microscope was used to study the morphology of the cryogel samples. Samples were placed on a glass slide and images were recorded at 20X and 40X magnification [35].

2.5. Cell Culture

The in vitro studies were conducted with spontaneously immortalized human keratinocyte cell line (HaCaT) (at the 20th-25th passages) which obtained from CLS 300493 (Germany). HaCaT cell lines were grown in Roswell Park Memorial Institute (RPMI) (Sigma-Aldrich, Germany). The culture medium was supplemented with 10% fetal bovine serum (FBS), 1% L-Glutamine (Biowest, Nuaillé, France) and 100 U/ml Penicillin/streptomycin (Hyclone, GE Healthcare, USA). The cells were incubated at 37°C in a 5% CO_2 incubator (IN55, Memmert, Germany). During the cell culture studies, all experiments were carried out in a laminar flow cabinet (DEMAIR, MSC-II A, Turkey).

2.6. Cultivation of HaCaT Cells on Cryogels

Before going through the cultivation of cells on cryogels, they were sterilized by immersing them into increasing concentrations of ethanol (60–100%) (v/v) for 60 min. Afterward, they were washed with sterile ultrapure water several times to remove ethanol. Prior to culturing the cells, sterile cryogel samples were kept in the medium at 37 °C for 3 h.

HaCaT cells were seeded on the cryogels with a density of 1×10^6 cells/sample [36]. For all in vitro analyses, the cryogels of identical dimensions (13 mm in diameter 0,5 mm in thickness) and dry weight (20 mg) were utilized [37]. The experimental groups include (i) control (only polystyrene-culture plate), (ii) PVA/Gel (*P. emblica* free cryogel), (iii) PVA/Gel/*P.emblica*-0.5 (0.5% of *P. emblica* loaded cryogel) (iv) PVA/Gel/*P.emblica*-1 (1% of *P. emblica* loaded cryogel), (v) PVA/Gel/*P.emblica*-1.5 (1.5% of *P. emblica* loaded cryogel) and (vi) PVA/Gel/*P.emblica*-2 (2% of *P. emblica* loaded cryogel).

2.7. MTT Assay

The MTT (3-[4,5-dimethylthiazol-2-yl]-2,5-diphenyltetrazolium bromide) was employed to assess the effect of *P. emblica* on cell viability and cytotoxicity in cryogels. MTT assay was preformed at 24, 48 and 72 h. After the incubation period, the cells incubated with MTT solution (0.5 mg/mL in PBS) for nearly 4 hours at 37 °C. Subsequently, DMSO was supplied to the wells to dissolve formazan crystals and placed on a shaker (Everlast Rocker 247, Benchmark, USA) for 30 min. The absorbance value of each well was measured using a spectrophotometer (Uvmini-1240, Shimadzu, Japan) at 570 nm. The formula of the percentage of cell viability was:

$$\text{Cell viability (\%)} = \frac{\text{Average OD570 of test cells}}{\text{Average OD570 of control cells}} \times 100 \quad (4)$$

 doi:10.20944/preprints202311.1288.v2

In this Equation, test cells indicate the viability of cells cultured on the cryogels, while control cells indicate the viability of cells cultured on culture plate.

2.8. Trypan Blue Exclusion Assay

The effect of the *P. emblica* on cell viability was evaluated by the trypan blue exclusion assay at 24, 48 and 72 h. After the incubation time, the cryogels were carefully scraped using scissors, and the cells were subsequently detached from the surface using trypsin. By dissolving the medium with the pellet, the cells and 0.4% trypan blue dye were mixed in ependorf at a ratio of 1:1. Number of viable cells was then counted with hemocytometer. The cell viability were calculated using Equation 5.

$$\text{Cell viability (\%)} = \frac{\text{Average viable cell count of test cells}}{\text{Average viable cell count of control cells}} \times 100 \qquad (5)$$

In Equation 5, the term "test cells" refers to the viable cells that were cultured on cryogels, whereas the term "control cells" refers to the viable cells that were cultured on a culture plate.

2.9. Live-Dead Staining Assay

The live/dead staining assay was performed to assess the activity of *P. emblica* loaded wound dressing materials on cell viability. After 72 hour cell were seeded on cryogels, 1 µM Calcein-AM (C-AM) and 1 µM Ethidium homodimer-1 (Eth-1) dyes were added. Following 30 minutes of incubation which is under room temperature and shielded from light, staining solutions were discarded from the wells and then rinsed with PBS. The stained cells on cryogel samples were viewed under a microscope at 20X magnification. The cell viability of cryogels were calculated using Equation 6.

Cell viability of cryogels (%) = Live cells / (Live cells + dead cells) x 100 (6)

2.10. Phase Contrast Microscopy

In order to monitorize the microscopic images of the synthesized cryogels, 13 mm diameter Thermanox coverslips (Thermo Fisher Scientific, Waltham, USA) were placed in the 24-well plate and then cryogels were synthesized onto them with a thickness of 0,5 mm. The cryogels were imaged 72 hours after cell cultivation. Images of the cells cultured in polystyrene-culture plate was used as a control to compare and evaluate the cells. The images of cryogels were obtained with phase contrast microscope (Leica, Dmil Led Fluo, Germany).

2.11. Giemsa Staining

Giemsa staining was performed to investigate the efficacy of *P. emblica* on HaCaT cell morphology. Cryogels were synthesized to form a thin layer on coverslips and cells were cultured on them. After 72 hours of incubation, the medium was removed and cells were treated with methanol for 15 minutes for fixation [38]. The cryogels were immersed in a 5% Giemsa staining solution for 30 minutes. Following the staining step, the cryogels were thoroughly washed with water to remove excess stain. The images of cells on cryogels were captured using an inverted microscope at a magnification of 20X.

2.12. Immunofluorescence Staining

Immunofluorescence staining was carried out to determine the effectiveness of the *P. emblica* loaded cryogels on keratinocyte morphology, adhesion, infiltration, cell-cell and cell-matrix interactions. The cells were seeded on the cryogels in a 24-well cell culture plate for 72 hours. For cell fixation, 4% (v/v) paraformaldehyde in PBS was added and incubated at room temperature for 30 minutes followed by washing with PBS. The samples were permeabilized with Triton-X 100 in PBS (0.1%; v/v) for at least 10 minutes. Alexa Fluor 594 phalloidin dye was prepared with 1% Bovine Serum Albumin (BSA; w/v) in PBS-T (PBS with Tween 20) at a 1/1000 ratio (v/v). Gap junctional protein (Connexin 43, Cx43) was detected under fluorescence microscope using a primary rabit anti-Cx43 antibody (ab230537, 1:500 dilution) with a secondary goat anti-rabbit IgG H&L antibody (Alexa Fluor® 488) (ab150077, 1:1000 dilution) [39]. In addition to staining the actin filaments of the cells,

 doi:10.20944/preprints202311.1288.v2

DAPI (4',6-diamidino-2-phenylindole) dye was employed to stain the cell nucleus. For this purpose, DAPI dye was prepared in PBS at a ratio of 1/1000 (v/v). Alexa Fluor 594 and DAPI staining solution were added to the fixed cells for 90 minutes in the dark at room temperature. After the incubation period, the staining solution was removed and rinsed with PBS. Finally, the cryogels were visualized at 20X magnification under a fluorescence microscope (Dmil Led Fluo, Leica, Germany). Also, imageJ software was used to analyses fluorescein signals in Cx43 images [40].

2.13. SEM Analysis

SEM analysis was performed to assess the effect of cryogels on HaCaT morphology. 72 hours after cell seeding, cells were fixed using 2.5% glutaraldehyde solution in PBS for 3 h at room temperature to preserve the cellular structures. The cryogel samples were rinsed with PBS and dehydrated with increasing concentrations of alcohol (30% to 100%). Cryogel samples were dried with lyophilizer and then coated with gold-palladium (2:3) prior to SEM imaging. The coated samples were loaded into the SEM chamber and imaged at 1000X and 2500X.

2.14. Statistical Analysis

All data were accomplished by Statistical Package for Social Sciences v20.0 software (SPSS, Chicago, IL, USA). Results were presented as mean ± standard deviation (SD) of values from three independent experiments. Statistical tests were conducted using GraphPad Prism 8.4.3 software (GraphPad Software, La Jolla, CA, USA). ImageJ software was used to analyses fluorescein signals. A two-way analysis of variance (ANOVA) and Tukey's test were utilized to compare data when three or more variables were present. Statistical differences were considered significant at $P < 0.05$.

3. Results and Discussion

3.1. Synthesis of Cryogels

The properties of five different PVA/Gel-based cryogels containing different amounts of *P. emblica* were investigated. When the *P. emblica* ratio in the cryogel was increased above 2%, it was observed that there was a deterioration in the structure of the cryogel. Therefore, *P. emblica* concentrations in the cryogel were selected as 0.5%, 1%, 1.5% and 2% final concentrations to ensure the stability and functionality of the cryogel. The cryogels synthesized in a 24-well plate had a diameter of 13 mm. As a result of the morphological examinations, it was observed that the cryogels were flexible, good mechanical strength porous and sponge-like structures. Images of cryogels synthesized within the scope of the study were given in Figure 2. It was observed that as the amount of *P. emblica* in the cryogels increased, it became slightly whiter.

 doi:10.20944/preprints202311.1288.v2

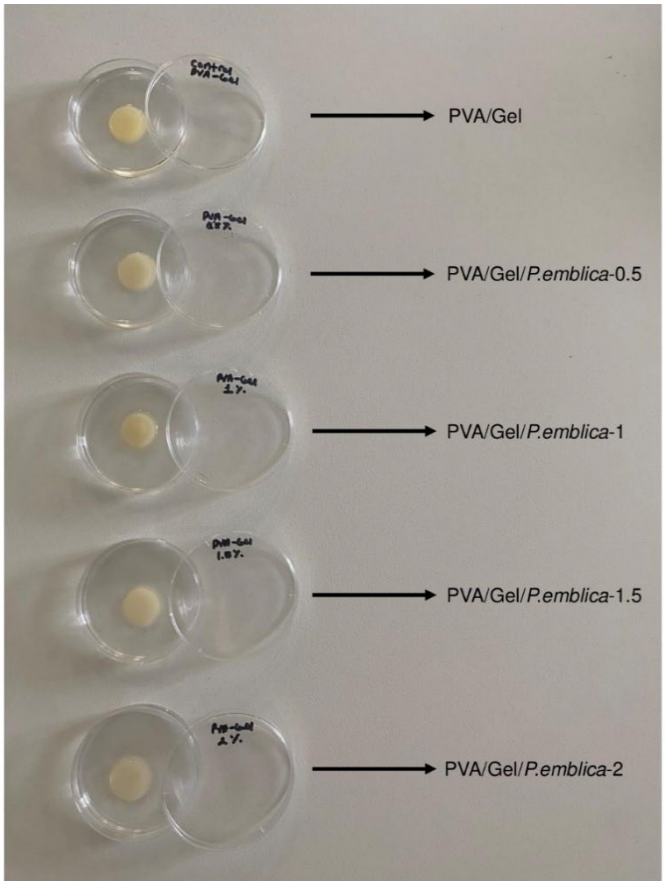

Figure 2. Images of synthesized cryogels.

3.2. Swelling Studies

The effect of *P. emblica* amounts on swelling rate, polymerization yield and porosity of cryogels were assessed by swelling tests. The swelling process is defined as the penetration of liquid molecules into the polymer network [41]. The high and rapid swelling capabilities of cryogels allow them to maintain a moist environment at the wound surface, prevent leakage of body fluids and absorb wound fluids; therefore, they are preferable for wound dressings. The synthesized cryogels exhibited a rapid and high swelling response when immersed in a liquid solution which is in line with the literature [42,43].

Within the first 15 minutes, the synthesized cryogels achieved the maximum swelling level and thus no change was observed in subsequent measurements and equilibrium was attained. Figure 3 showed the image of the cryogels dried with a lyophilizer.

 doi:10.20944/preprints202311.1288.v2

Figure 3. Dried cryogels.

The swelling rate, polymerization yield and macroporosity of the cryogels were obtained from swelling tests and the results were summarized in Table 1.

Table 1. Swelling properties of cryogels.

	Swelling Rate (%)	Polymerization Yield (%)	Macroporosity (%)
PVA/Gel	450 ± 4.7	92 ± 2.1	82 ± 2.1
PVA/Gel/*P.emblica*-0.5	452 ± 1.2	93 ± 0.6	82 ± 1
PVA/Gel/*P.emblica*-1	457 ± 2.5	92 ± 1.2	82 ± 2
PVA/Gel/*P.emblica*-1.5	458 ± 2.6	93 ± 1	83 ± 1.2
PVA/Gel/*P.emblica*-2	446 ± 5.5	91 ± 2.5	81 ± 3.5

The swelling ratio of cryogel samples is an important parameter that indicates the extent to which they absorb water or swell when immersed in a liquid medium. As can be seen in Table 1, all cryogel samples, including the control, exhibited high swelling ratios ranging from 446% to 458%. The swelling ratio of PVA/Gel, PVA/Gel/*P.emblica*-0.5, PVA/Gel/*P.emblica*-1, PVA/Gel/*P.emblica*-1.5, PVA/Gel/*P.emblica*-1.5, PVA/Gel/*P.emblica*-2 cryogels were calculated as 450% ± 4.7%, 452% ± 1.2%, 457% ± 2.5%, 458% ± 2.6% and 446% ± 5.5% respectively. According to these results, there were slight changes in swelling rate with the addition of *P. emblica* extract at different concentrations. Cryogel containing 1.5% *P.emblica* extract (PVA/Gel/*P.emblica*-1.5) displayed the highest swelling ratio. When *P. emblica* is added to the cryogel, the hydrophobic components in the *P. emblica* interact with the

 doi:10.20944/preprints202311.1288.v2

cryogel material. These interactions can change the properties of the cryogel, thereby increasing the area available for water adsorption within the cryogel network. The increase in *P. emblica* resulted in the formation of cryogel with larger pores and increased swelling ratio. On the other hand, PVA/Gel/*P.emblica*-2 cryogel showed the lowest swelling rate. This may be due to the 2% *P. emblica* increased the hyhrophobic character of the cryogels and the water uptake ratio decreased slightly.

The polymerization yield is a measure of the efficiency of the polymerization process and indicates how much of the monomer material is converted into the final cryogel. It was calculated with equation 2. The yield of the polymerization of PVA/Gel, PVA/Gel/*P.emblica*-0.5, PVA/Gel/*P.emblica*-1, PVA/Gel/*P.emblica*-1.5, PVA/Gel/*P.emblica*-1.5, PVA/Gel/*P.emblica*-2 cryogels was calculated as 92% ± 2.1%, 93% ± 0.6%, 92% ± 1.2%, 93% ± 1% and 91% ± 2.5%, respectively. Polymerization yields were found to be high in compatible with the other studies [44,45]. The data show that a slightly higher yield was achieved when the amount of *P. emblica* was increased.

The porosity of cryogels is one of their most important features for tissue engineering applications. The interconnected pores provide a large surface area for cell adhesion, proliferation, and nutrient diffusion. The synthesized cryogels showed a high amount of porous structure in accordance with the literature [46]. The macroporosities were calculated as 82% ± 2.1%, 82% ± 1%, 82%± 2%, 83% ± 1.2% and 81% ± 3.5% for PVA/Gel, PVA/Gel/*P.emblica*-0.5, PVA/Gel/*P.emblica*-1, PVA/Gel/*P.emblica*-1.5, PVA/Gel/*P.emblica*-1.5, PVA/Gel/*P.emblica*-2, respectively.

Based on the results of the swelling tests, the synthesized cryogels exhibit excellent macroporosity and swelling rate. The swelling properties of cryogels are associated with mimicking the ECM with features such as oxygen migration, diffusion of molecules, cell adhesion that the wound dressing materials meet. Accordingly, it was concluded that *P. emblica* loaded cryogels are suitable as wound dressings [43,47].

3.3. BET Analysis

The BET analysis was performed to utilize for determining the surface area of cryogels. The BET analysis results of PVA/Gel, PVA/Gel/*P.emblica*-0.5, PVA/Gel/*P.emblica*-1, PVA/Gel/*P.emblica*-1.5, PVA/Gel/*P.emblica*-2 cryogels were determined as 18 m^2/g, 18 m^2/g, 20 m^2/g, 21 m^2/g, 20 m^2/g. BET analysis obtained in three replicates are provided with their standard deviations. Overall, the results showed that the addition of *P. emblica* extract to cryogels slightly increased their specific surface area. Cryogels with higher surface area offer more attachment for cells, promoting cell adhesion and proliferation. This can result in better compatibility and combination with living tissue [48].

3.4. Morphology Analysis

In biomaterial applications, a porous structure is required for the polymeric material to be compatible with cell growth [49]. The macroporous structure of the cryogels were evaluated using SEM and optical microscopy. In this thesis, cryogels used for SEM analyzes were first frozen at -20˚C and then dried with a lyophilizer. In Figure 4, the internal morphology of each cryogel sample was visualized by SEM. The PVA/Gel and *P. emblica* loaded PVA/Gel cryogels possess similar structures and pore sizes of 30-120 μm and 30-100 μm, respectively. The diameter of HaCaT cells varies between 20-25 micrometer [50]. Considering the size of the Hacat cell, the pore size was sufficient for the cell to settle. Moreover, SEM results displayed that the synthesized cryogels had an dense, thin and interconnected pore morphology and a macroporous structure. This macroporous structure makes the cryogel appear opaque. The macroporous polymeric structure of the cryogel is suitable to serve as a scaffold for cell adhesion, proliferation, and migration [51–53]. In addition, the morphological surface properties of the synthesized cryogels were visualized using optical microscope images (Figure 5). Although increasing amounts of four different *P. emblica* concentrations were used to synthesize the cryogels, *P. emblica* did not significantly affect the macroporous morphological structure and surface matrix of the cryogels.

 doi:10.20944/preprints202311.1288.v2

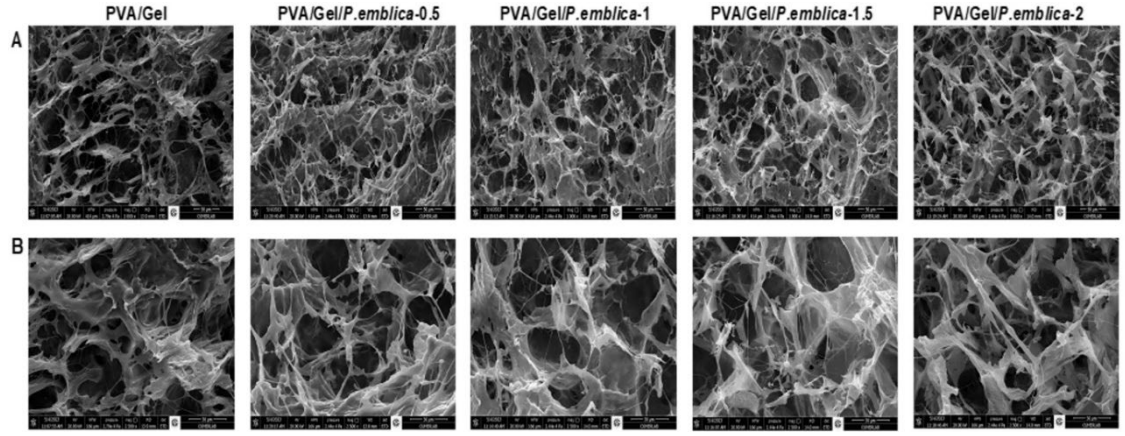

Figure 4. The surface and structures of cryogels without cells by scanning electron microscopy (SEM). SEM images images taken **(A)** at 1000X magnification, scale bar: 50 μm and **(B)** at magnification 2500X, scale bar: 30 μm.

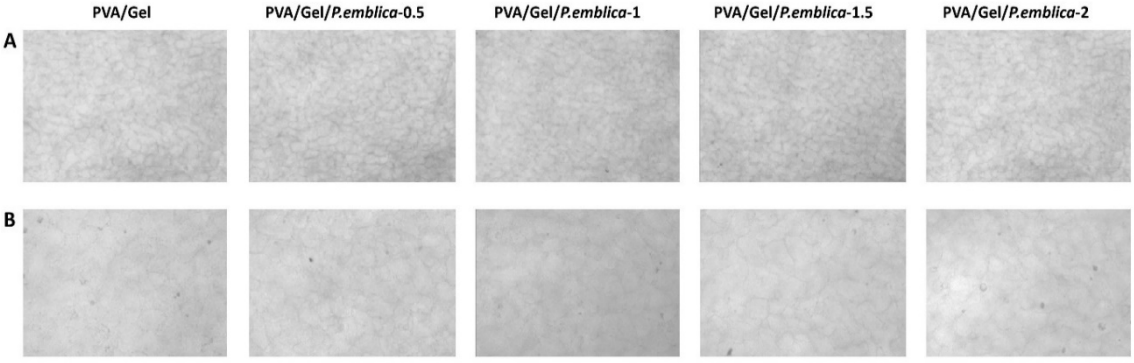

Figure 5. The surface morphology of PVA/Gel, PVA/Gel/*P.emblica*-0.5, PVA/Gel/*P.emblica*-1, PVA/Gel/*P.emblica*-1.5 and PVA/Gel/*P.emblica*-2 cryogels without cells by optical microscope. Optical microscope images taken **(a)** at 20X magnification, scale bar: 100 μm and **(b)** at magnification 40X, scale bar: 50 μm. PVA/Gel: Poly (vinyl alcohol)/Gelatin cryogels; PVA/Gel/*P.emblica*: *P. emblica* loaded PVA/Gel cryogels; *P. emblica*: *Phyllanthus emblica*.

3.5. Assessment of Cell Viability of Cryogels by MTT Assay, Trypan Blue Exclusion Assay and Live/Dead Staining

The cytotoxic impact of PVA/Gel, PVA/Gel/*P.emblica*-0.5, PVA/Gel/*P.emblica*-1, PVA/Gel/*P.emblica*-1.5 and PVA/Gel/*P.emblica*-2 cryogels on keratinocytes was investigated by the MTT assay at 24th, 48th and 72nd hour (Figure 6). The cell viability in the control significantly increased by 40.7% at 48th hour compared to 24th hour, but decreased by 4.22% at 72nd hour as compared to the 48th hour ($P< 0.0001$, $P= 0.0663$). Also, the cell viability in PVA/Gel cryogel significantly increased by 29.78% and decreased by 6.99%, respectively ($P< 0.0001$, $P= 0.0006$). In PVA/Gel/*P.emblica*-0.5 cryogel, it increased significantly by 46.98% and 15.53%, respectively. ($P< 0.0001$, $P= 0.0006$). In PVA/Gel/*P.emblica*-1 cryogel it increased significantly by 48.26% and 17.73%, respectively ($P< 0.0001$, $P= 0.0133$). In PVA/Gel/*P.emblica*-1.5 cryogel, it increased significantly as 52.33% and 14.47%, respectively ($P< 0.0001$, $P= 0.0049$). In PVA/Gel/*P.emblica*-2 cryogel, it increased significantly as 34.32% and 6.92%, respectively ($P< 0.0001$, $P= 0.0272$) (Figure 6a).

 doi:10.20944/preprints202311.1288.v2

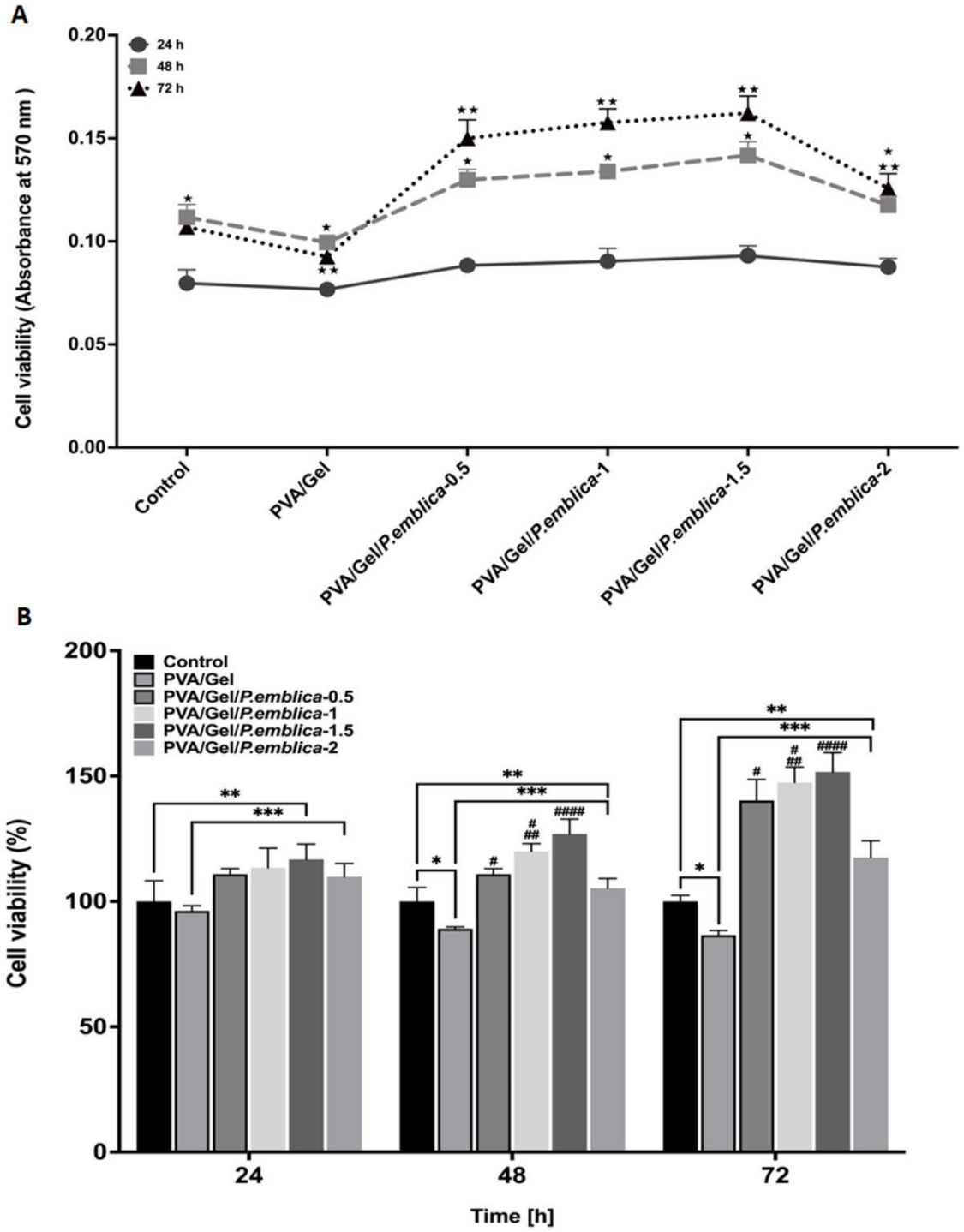

Figure 6. Determination of cytotoxic effect of PVA/Gel and PVA/Gel/*P.emblica* cryogels by MTT assay. The viability of HaCaT cell line on cryogels was assessed by MTT assay at 24, 48, and 72 hour. Cell cultured in polystyrene-culture plate was used as a control**. (A)** Quantitative evaluation of cell viability. The amount of MTT-formazan was determined by 570 nm absorbance as the wavelength. (**B)** Cell viability (%) of keratinocytes on cryogels compared with the control. The control cells were considered to have 100% survival. The histograms illustrate the percentage of viable cells, relative to the control cells. Three measurements were conducted from each well, and the data was reported as the mean± standard deviation (SD). Tukey test and One-ANOVA were conducted for statistical analysis. *P< 0.05 is significantly different from 24 h. **P< 0.05 is significantly different from 48 h. *P< 0.05 and **P< 0.05 are significantly different from control. ***P< 0.05 is significantly different from PVA/Gel. $^{\#}$P< 0.05 is significantly different from PVA/Gel/*P.emblica*-2. $^{\#\#}$P< 0.05 is significantly

 doi:10.20944/preprints202311.1288.v2

different from PVA/Gel/*P.emblica*-0.5. ###P< 0.05 is significantly different from other PVA/Gel/*P.emblica* cryogels. PVA/Gel: Poly (vinyl alcohol)/Gelatin cryogels; PVA/Gel/*P.emblica*: *P. emblica* loaded PVA/Gel cryogels; *P. emblica*: *Phyllanthus emblica*; MTT: (3-(4,5-dimethylthiazol-2) 2,5-diphenyltetrazolium bromide; SD: Standard deviation.

In comparision with the control, cell proliferation was decreased in the PVA/Gel cryogel by 3.77% ± 2.05%, 10.90% ± 0.75%, and 13.47% ± 1.86% at 24th, 48th and 72nd, respectively (P= 0.2530, P= 0.0049, P= 0.0001, respectively). On the other hand, cell proliferation in PVA/Gel/ *P.emblica*-0.5 showed an increase of 10.88% ± 2.20%, 10.88% ± 2.20%, and 40.25 ± 8.36%, respectively, compared to control (P= 0.0380, P= 0.0076, P< 0.0001, respectively). The cell proliferation was higher in PVA/Gel/*P.emblica*-1 cryogel by 13.39% ± 7.85%, 19.93% ± 3.10%, and 47.42 ± 6.16%, respectively, compared to control (P= 0.0185, P= 0.0008, P< 0.0001, respectively). The cell proliferation was increased in PVA/Gel/*P.emblica*-1.5 cryogel by 16.74% ± 6.10%, 26.87% ± 5.96% and 51.63 ± 7.74%, respectively, compared to control (P= 0.0171, P= 0.0013, P< 0.0001, respectively). The cell proliferation was significantly increased in PVA/Gel/*P.emblica*-2 cryogel by 9.83% ± 5.31%, 5.25% ± 3.89% and 17.50 ± 6.68%, respectively, compared to control (P= 0.0574, P= 0.2082, P= 0.0039, respectively).

According to MTT assay, cell proliferation in PVA/Gel/*P.emblica*-0.5 cryogel was 15.22%, 24.44% and 62.09% higher at 24, 48 and 72 h, respectively, compared to PVA/Gel (P= 0.0003, P< 0.0001, P< 0.0001). Moreover, the cell proliferation was increased in the PVA/Gel/*P.emblica*-1 cryogel compared to PVA/Gel by 17.83%, 34.60% and 70.37% (P= 0.0014, P< 0.0001, P< 0.0001). The cell proliferation was significantly increased in the PVA/Gel/*P.emblica*-1.5 cryogel compared to PVA/Gel by 21.30%, 42.38% and 75.24% (P= 0.0005, P< 0.0001, P< 0.000l). Also, the cell proliferation was 14.13%, 18.12% and 35.79% higher in the PVA/Gel/*P.emblica*-2 cryogel compared to PVA/Gel by (P= 0.0011, P= 0.0002, P= 0.0002, respectively).

According to MTT assay, the cell proliferation in the PVA/Gel/*P.emblica*-1, PVA/Gel/*P.emblica*-1.5 *and* PVA/Gel/*P.emblica*-2 cryogels showed increases of 2.26%, 5.28% and -0.94% at 24 hour, respectively, compared to PVA/Gel/*P.emblica*-0.5 (P= 0.5198, P= 0.0958, P= 0.07148). In addition, the cell proliferation significantly increased at 48 h and 72 h by 8.17%, 14.42%, -5.07% and 5.11%, 8.11%, -16.22% (P= 0.0016 P= 0.0008, P= 0.0187 for 48th hour and P= 0.0252, P= 0.0066, P= 0.00297 for 72nd h). Moreover, the cell proliferation was increased in the PVA/Gel/*P.emblica*-1.5 *and P.emblica*-2 cryogel compared to PVA/Gel/*P.emblica*-1 cryogel by 2.95% and -3.14% respectively at 24th h (P= 0.5232, P= 0.3486). Also, the cell proliferation significantly increased at 48th and 72nd hours by 5.78%, -12.24% and 2.85%, -20.30% (P= 0.0479, P= 0.0001 for 48th hour and P= 0.0379, P= 0.0010 for 72nd hour, respectively). Also, the cell proliferation was decreased in the PVA/Gel/*P.emblica*-2 cryogel compared to PVA/Gel/*P.emblica*-1.5 by -5.91%, 17.04%, 22.51% respectively at 24, 48, 72 hours (P= 0.967, P= 0.0005, P= 0.0014, respectively) (Figure 6b).

Trypan blue assay was performed to investigate the efficacy of PVA/Gel, PVA/Gel/*P.emblica*-0.5, PVA/Gel/*P.emblica*-1, PVA/Gel/*P.emblica*-1.5 and PVA/Gel/*P.emblica*-2 cryogels on keratinocytes viability at 24th, 48th and 72nd h (Figure 7). In comparision with control, the cell number of PVA/Gel cryogel was declined by 7.23% ± 8.45%, 7.84% ± 3.81%, and 10.94% ± 3.47%, respectively (P= 0.0913, P= 0.0471, P= 0.0641 respectively). Moreover, the cell number in the PVA/Gel/*P.emblica*-0.5 cryogel was significantly increased by 11.45% ± 7.69%, 20.41% ± 2.3%, and 39.29 ± 4.72%, respectively, compared to control (P= 0.0177, P< 0.0001, P= 0.0003, respectively). Also, the cell number in the PVA/Gel/*P.emblica*-1 cryogel was increased by 31.93% ± 10.36%, 43.71% ± 3.94%, and 40.85 ± 2.31%, respectively, compared to control (P= 0.0002, P< 0.0001, P= 0.0001, respectively). The cell number in the PVA/Gel/*P.emblica*-1.5 cryogel was significantly increased by 48.19% ± 4.88%, 56.08% ± 4.10% and 67.63 ± 3.83%, respectively, compared to control (P< 0.0001 for all). The cell number in the PVA/Gel/*P.emblica*-2 cryogel was significantly increased by 1.41% ± 2.69%, 8.87% ± 2.07% and 10.71 ± 4.99%, respectively, compared to control (P= 0.0585, P= 0.0013, P= 0.0393, respectively).

 doi:10.20944/preprints202311.1288.v2

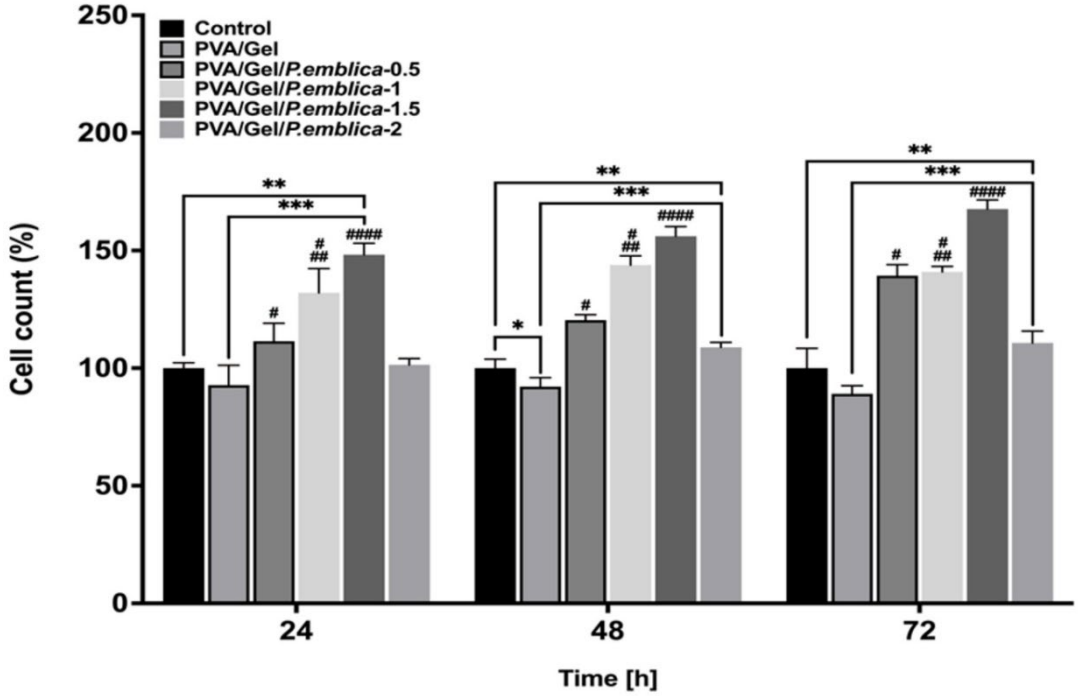

Figure 7. The efficacy of PVA/Gel and PVA/Gel/*P.emblica* cryogels on number of viable cells. The viability of HaCaT cell line on cryogels was assessed by trypan blue exclusion assay at 24, 48 and 72 hours. Cell cultured in polystyrene-culture plate was utilized as a control. Three measurements were conducted from each well, and the data was reported as the mean± standard deviation (SD). Statistical analysis was performed using the Tukey and One-way ANOVA tests. *P< 0.05 and **P< 0.05 are significantly different from control. ***P< 0.05 is significantly different from PVA/Gel. #P< 0.05 is significantly different from PVA/Gel/*P.emblica*-2. ##P< 0.05 is significantly different from PVA/Gel/*P.emblica*-0.5. ###P< 0.05 is significantly different from other PVA/Gel/*P.emblica* cryogels. PVA/Gel: Poly (vinyl alcohol)/Gelatin cryogels; PVA/Gel/*P.emblica*: PVA/Gel cryogels based loaded with *P. emblica*; *P. emblica*: *Phyllanthus emblica*; SD: Standard error.

According to trypan blue assay, the number of cells in the PVA/Gel/*P.emblica*-0.5 cryogel was increased by 20.13%, 30.65% and 56.39% at 24, 48 and 72 hours compared to PVA/Gel, respectively (P= 0.0061, P< 0.0001, P< 0.0001). The number of cells was 42.21%, 55.93% and 58.15% higher in PVA/Gel/*P.emblica*-1 cryogel compared to PVA/Gel (P= 0.0004, P< 0.0001, P< 0.0001). The cell number was significantly increased in the PVA/Gel/*P.emblica*-1.5 cryogel compared to PVA/Gel by 59.74%, 69.35% and 88.22% (P< 0.0001, for all). In addition, the number of cells was 9.31%, 18.12% and 24.31% higher in the PVA/Gel/*P.emblica*-2 cryogel compared to PVA/Gel (P= 0.0766, P= 0.0007, P= 0.0005, respectively).

According to trypan blue assay, the viable cell number was significantly increased in the other PVA/Gel/*P.emblica*-1, PVA/Gel/ *P.emblica*-1.5 *and* PVA/Gel/ *P.emblica*-2 cryogels compared to PVA/Gel/*P.emblica*-0.5 by 18.38%, 32.97% and -9.01%, respectively at 24 h (P= 0.0139, P= 0.0002, P= 0.0379). In addition, the cell number significantly increased at 48 and 72 hours by 19.35%, 29.62%, -9.59% and 1.12%, 20.35%, -20.51% (P< 0.0001, P< 0.0001, P= 0.0006 for 48 h and P= 0.4492, P= 0.0003, P= 0.0008 for 72 h). Furthermore, the cell number in the PVA/Gel/*P.emblica*-1.5 *and* PVA/Gel/*P.emblica*-2 cryogel showed significant increases of 12.33% and -23.14% compared to PVA/Gel/*P.emblica*-1 cryogels at 24 hour, respectively (P= 0.0047, P= 0.0004). Also, the cell number significantly increased at 48 and 72 hours by 8.61%, -24.25% and 19.02%, -21.39% (P= 0.0024, P< 0.0001 for 48 h and P< 0.0001, P< 0.0001 for 72 h). Also, the cell number was significantly decreased in the PVA/Gel/*P.emblica*-2 cryogel compared to PVA/Gel/*P.emblica*-1.5 by 31.57%, 30.25%, 33.95% at 24, 48, 72 h, respectively (P< 0.0001 for all).

 doi:10.20944/preprints202311.1288.v2

A live/dead assay was performed to evaluate the cell viability of cells, where green fluorescence indicated viable cells and red fluorescence indicated dead cells. (Figure 8). Cells were seeded on PVA/Gel, PVA/Gel/*P.emblica*-0.5, PVA/Gel/*P.emblica*-1, PVA/Gel/*P.emblica*-1.5 and PVA/Gel/*P.emblica*-2 cryogels for 24th, 48th and 72nd h. As seen in Figure 8a–c relatively similar numbers were determined in live and dead cells cultured in control and PVA/Gel/*P.emblica*-0.5, PVA/Gel/*P.emblica*-1, PVA/Gel/*P.emblica*-1.5 and PVA/Gel/*P.emblica*-2 cryogels for all hours. The cells cultured on the PVA/Gel *P.emblica*-0.5, PVA/Gel/*P.emblica*-1, PVA/Gel/*P.emblica*-1.5 and PVA/Gel/*P.emblica*-2 cryogels exhibited a higher percentage of green fluorescence, which indicates viable cells compared to the PVA/Gel. The majority of cells cultured on the PVA/Gel/*P.emblica*-0.5, PVA/Gel/*P.emblica*-1, PVA/Gel/*P.emblica*-1.5 and PVA/Gel/*P.emblica*-2 cryogels emitted green fluorescence, which indicates a high level of cell viability and cell proliferation. As shown in 8a, 8b and 8c, the addition of *P. emblica* extract to the PVA/Gel cryogels did not adversely affect cell viability relative to the live/dead assay. The percentage of viable (green) cells was higher in cultured in cryogels loaded with *P. emblica*. Unlike controls, cells cultivated especially in PVA/Gel/*P.emblica*-0.5, PVA/Gel/*P.emblica*-1, PVA/Gel/*P.emblica*-1.5 cryogels showed viable (green) cells with more rounded contours. In addition, compared to PVA/Gel cryogels, PVA/Gel/*P.emblica*-0.5, PVA/Gel/*P.emblica*-1, PVA/Gel/*P.emblica*-1.5 and PVA/Gel/P.emblica-2 cryogels have more viable cells.

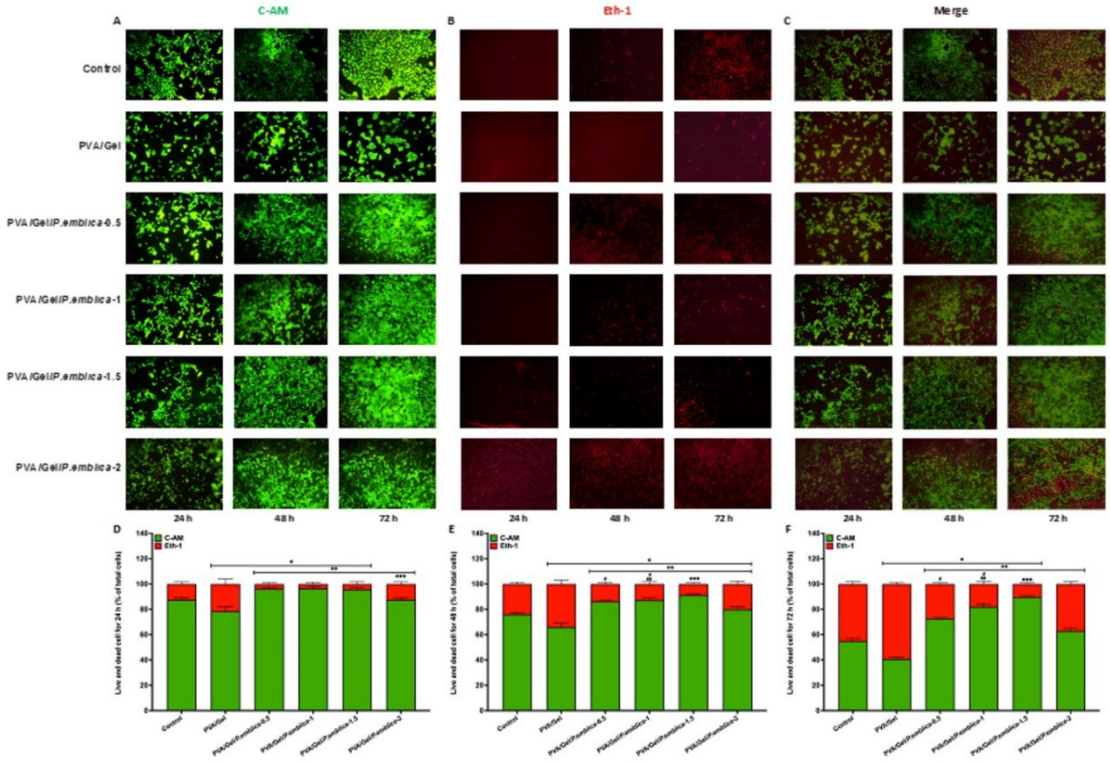

Figure 8. Determination of cell viability of PVA/Gel and PVA/Gel/*P.emblica* cryogels by live/dead staining. Live-dead assay was performed at 24, 48 and 72 hours. Cell cultured in polystyrene-culture plate was utilized as a control. Fluorescent microscope images showed cells on PVA/Gel, PVA/Gel/*P.emblica*-0.5, PVA/Gel/*P.emblica*-1, PVA/Gel/*P.emblica*-1.5 and PVA/Gel/*P.emblica*-2 cryogels stained with **(A)** C-AM (green fluorescent) and **(B)** Eth-1 (red fluorescent) and **(C)** both C-AM and Eth-1 to obtain merged images (Scale bar: 100 µm). The quantitative data for live and dead cells was obtained using the live/dead assay at **(D)** 24 h, **(E)** 48 h, **(F)** 72 h. Cryogels were visualized and analyzed using a microscope and ImageJ software. The data are expressed as the total percentage of live and dead cells, accompanied by the mean ± standard deviation (SD). Statistical analysis was conducted using the Tukey test and One-way ANOVA. *P< 0.05 is significantly different from control. **P< 0.05 is significantly different from PVA/Gel. ***P< 0.05 is significantly different from other PVA/Gel/*P.emblica* cryogels. #P< 0.05 is significantly different from PVA/Gel/*P.emblica*-2. ##P< 0.05 is significantly different from PVA/Gel/*P.emblica*-0.5. C-AM: Calcein Acetomethoxy; Eth-1:

 doi:10.20944/preprints202311.1288.v2

Ethidium homodimer-1; PVA/Gel: Poly (vinyl alcohol)/Gelatin cryogels; PVA/Gel/*P.emblica*: *P. emblica* loaded PVA/Gel cryogels; *P. emblica*: *Phyllanthus emblica*; SD: Standard deviation.

According to live/dead assay, viable cells in the PVA/Gel cryogel decreased by 11.81% ± 1.38%, 12.86% ± 1.72%, and 25.77% ± 2.16% at 24, 48, and 72 hours compared to control, respectively (P= 0.0288, P= 0.0145, P= 0.0008). The viable cell ratio in PVA/Gel/*P.emblica*-0.5 was significantly increased by 10.48% ± 3.97%, 14.86% ± 2.74%, 34.05% ± 1.37% respectively cryogel compared to control (P= 0.0004, P= 0.0008, P< 0.0001). Also, the viable cell ratio in PVA/Gel/*P.emblica*-1 cryogel was significantly increased by 10.67% ± 1.03%, 17.07% ± 1.86% and 52.76% ± 0.75% respectively cryogel compared to control (P= 0.0002, P= 0.0034, P= 0.0001). Also, the viable cell ratio in PVA/Gel/*P.emblica*-1.5 cryogel was significantly increased by 9.33% ± 1.17%, 21.95% ± 1.79%, 66.87% ± 2.61% 10.06 respectively cryogel compared to control (P= 0.0060, P= 0.0004, P< 0.0001). Also, the viable cell ratio in PVA/Gel/*P.emblica*-2 cryogel was significantly enhanced by 1.52% ± 1.37%, 5.99% ± 1.03%, 15.03% ± 1.63%, respectively cryogel compared to control (P> 0.9999, 0.0342, P> 0.9999). Moreover, the viable cells in the PVA/Gel/*P.emblica*-0.5 cryogel increased significantly by 25.27%, 31.38% and 80.58%, respectively compared to PVA/Gel (P= 0.0042, P= 0.0017, P< 0.0001). Also, the viable cells in the PVA/Gel/*P.emblica*-1 cryogel increased by 25.49%, 34.35% and 105.79%, respectively compared to PVA/Gel (P= 0.0026, P= 0.0005, P< 0.0001). The viable cells in the PVA/Gel/*P.emblica*-1.5 cryogel increased by 23.97%, 39.95% and 129.79%, respectively compared to PVA/Gel (P= 0.0069, P= 0.0003, P< 0.0001). The viable cells in the PVA/Gel/*P.emblica*-2 cryogel increased significantly by 15.12%, 21.63% and 54.96%, respectively compared with PVA/Gel (P= 0.0361, 0.0036, P= 0.0002).

According to live/dead assay, dead cells in the PVA/Gel cryogel increased by 82.67% ± 1.38%, 38.93 % ± 1.72%, and 30.66 % ± 2.16% at 24, 48, and 72 hours, respectively, compared to control (P= 0.0288, P= 0. 0145, P= 0.0008). Furthermore, the dead cell ratio in PVA/Gel/*P.emblica*-0.5 was decreased significantly by 73.33% ± 3.97%, 44.97% ± 2.74%, and 40.51% ± 1.37%, respectively cryogel compared to control (P= 0.0004, P= 0.0008, P< 0.0001). Also, the dead cell ratio in PVA/Gel/*P.emblica*-1 was significantly decreased by 74.67% ± 1.17%, 51.68% ± 1.86%, and 62.77% ± 0.75%, respectively compared to control (P= 0.0002, P= 0.0034, P= 0.0001). Moreover, the dead cell ratio in PVA/Gel/*P.emblica*-1.5 was significantly decreased by 65.33% ± 1.17%, 66.44% ± 1.79%, and 79.56% ± 2.61%, respectively cryogel compared to control (P= 0.0060, P= 0.0004, P< 0.0001). The dead cell ratio in PVA/Gel/*P.emblica*-2 was decreased by 10.67% ± 1.37%, 18.12% ± 1.03%, and 17.88% ± 1.63%, respectively cryogel compared to control (P> 0.9999, P= 0.0342, P> 0.9999). The dead cells in the PVA/Gel/*P.emblica*-0.5 cryogel decreased significantly by 85.40%, 60.39% and 54.47%, respectively compared to PVA/Gel (P= 0.0042, P= 0.0017, P< 0.0001). Also, the dead cells in the PVA/Gel/*P.emblica*-1 cryogel declined by 86.13%, 65.22% and 71.51%, respectively compared to PVA/Gel (P= 0.0026, P= 0.0005, P< 0.0001). Moreover, the dead cells in the PVA/Gel/*P.emblica*-1.5 cryogel decreased significantly by 81.02%, 75.85% and 84.36%, respectively compared to PVA/Gel (P= 0.0069, P= 0.0003, P< 0.0001). The dead cells in the PVA/Gel/*P.emblica*-2 cryogel declined significantly by 51.09%, 41.06% and 37.15%, respectively compared with PVA/Gel (P= 0.0361, P= 0.0036, P= 0.0002) (Figure 8d–f).

Cell scaffolds must be mechanically stable, biocompatible, biodegradable, but also porous with good interconnectivity for cell viability, proliferation, migration and other metabolic needs [51]. PVA is a synthetic polymer widely used to produce macroporous, spongy matrices in tissue engineering applications due to its biocompatibility, non-carcinogenic and non-toxic properties [54]. Gel is frequently preferred in biomaterial synthesis as an attractive natural polymer with its chemical structure, biocompatibility, and biodegradability properties that increase cell adhesion [55,56]. However, studies have revealed that biocompatible PVA and Gel-based scaffolds maintain the functionality of cells metabolically thanks to their strong, elastic and porous 3D structure, at the same time they support cell viability, adhesion, proliferation, mobility and allow the absorption of the necessary substrate for cell nutrition. For these reasons, it has been reported to be a promising platform in tissue engineering. Pterostilbene-loaded PVA/Gel cryogels have been reported as a potential dressing material in wound therapy, promoting cell viability and proliferation [57–59]. However, it has been reported that PVA/Gel cryogel promotes the viability and proliferation of endothelial cells and is particularly suitable for vascular tissue engineering applications [59]. In

 doi:10.20944/preprints202311.1288.v2

addition, it was determined that there was no cytotoxic effect for human skin cells cultured in PVA/Gelatin cryogel and the scaffold exhibited good biocompatibility [43]. The antioxidant, antidiabetic, anti-inflammatory, antiaging, wound healing, cryoprotective and hepatoprotective activities of *P. emblica* extracts used in traditional medicine were studied [25–27]. In in vitro studies, it has been reported that *P. emblica* extract promotes wound healing by supporting endothelial cells, fibroblast, and keratinocyte vitality, proliferation, migration, and angiogenesis through its high bioactive component content [28–30]. In addition, it has been shown in an in vivo animal model that *P. emblica* treatment increases tissue regeneration by reducing oxidative stress in the wound area, inducing collagen expression and angiogenesis [31,60]. In a different study, the potential of using the spray solution prepared with polyvinylpyrrolidone solution containing silver nanoparticles and *P. emblica* extract as an antibacterial, antioxidant and biocompatible wound dressing for fibroblasts and keratinocytes was demonstrated [61]. In addition, green tea, ginger, and *P. emblica* extracts loaded hydrgel have been reported to treat acne and accelerate wound healing in humans [62]. However, to the best of our knowledge, the effect of *P. emblica* binding to cryogel on cytotoxicity and its potential in tissue regeneration as a wound dressing are not yet known. Evaluation of cell viability and proliferation in the microenvironment as an indicator of biocompatibility in synthesized scaffold structures is very important in tissue engineering applications [62,63]. Therefore, in our study, for the first time in the literature, cell viability, and proliferation were evaluated after different incubation times with MTT and trypan blue exclusion assay in cells cultured in PVA/Gel cryogels to which different concentrations of *P. emblica* were added. In addition, live/dead assay was applied to visualize live and dead cells in culture medium to understand the effect of scaffolds on cell behavior [40,63].

In our study, the MTT test showed that cells were viable in PVA/Gel and PVA/Gel/*P.emblica* cryogels. Furthermore, a highly increased cellular metabolic activity was observed over time in cryogels with different concentrations of *P.emblica*. However, in the control, although the cell viability increased until the 2nd day of the cell culture, the cell viability decreased. This may be due to the rapid confluence of cells in the flat culture system compared to the 3D culture system, as the doubling time of the HaCaT cell is about 26.4-48 h [64,65]. Cells in monolayer culture with limited substrate area proliferate rapidly until they are confluent, but when the limit is reached, cell viability decreases due to contact inhibition [66]. In agreement with the characterization study data, the 3D macroporous structure, high swelling rate, pore sizes, the large surface area of the PVA/Gel/*P.emblica* cryogels were sufficient to facilitate the diffusion of macromolecules necessary for the metabolic activity of the cells and the removal of wastes. In this way, unlike the 2D culture medium, cell viability and proliferation continuously increased in PVA/Gel/*P.emblica* cryogels until the end of the 3rd day of culture, so that the cells filled the pores of the matrix [67]. Also, the increase in cell viability and proliferation was very limited in PVA/Gel cryogels compared to containing *P. emblica* cryogels. It has been reported in the literature that high antioxidant activity originating from bioactive secondary compounds reduces intracellular oxidative stress and increases cell viability [28,30,68]. It is known that *P. emblica* has strong antioxidant activity mainly due to the presence of phenolics, flavonoids and various gallic acid derivatives [27,29,69]. This high bioactive capacity of *P. emblica* may have promoted the viability and proliferation of cells cultured in cryogels. Similarly, in agreement with the MTT assay data, the trypan blue exclusion test confirmed that PVA/Gel/*P. emblica* cryogels provide a biosafe environment that promotes cell viability and increase in number. More importantly, the live/dead assay results confirmed other results from direct cytotoxicity studies by providing visible evidence that the *P. emblica* extract, together with the polymers used in the manufacture of cryogels, promotes cell viability by a functionally significant difference. These results demonstrate the high potential of the macroporous scaffold synthesized with natural *P. emblica* extract as a suitable dressing material with its good biocompatibility.

3.6. Investigation of Cell Morphology, Adhesion, Viability, Cell-Cell and Cell-Matrix Interactions on Cryogels via Phase Contrast Microscopy, Giemsa Staining, Immunofluorescence Staining and SEM

 doi:10.20944/preprints202311.1288.v2

Cells secrete ECM proteins in response to chemical-mechanical signals through their receptors and exhibit a characteristic morphology [70]. Cell-cell and cell-cryogel interaction can be investigated by using microscopic imaging of features such as focal adhesion of the cell, cytoskeleton with fluorophores, and nuclear distribution. [71]. Microscopic examination, giemsa, F-Actin/DAPI and Calcein-AM/Eth-1 staining was performed to assess the proliferation and morphology of cells cultured on control, PVA/Gel, PVA/Gel/*P.emblica*-0.5, PVA/Gel/*P.emblica*-1, PVA/Gel/*P.emblica*-1.5 and PVA/Gel/*P.emblica*-2 cryogels at 72nd h [72] (Figure 9). Phase contrast microscopy and giemsa staining showed that the cells adhered to the surface of the cryogels and penetrated the pores. Moreover, especially in the PVA/Gel/*P.emblica* cryogels, cells proliferated extensively, forming large-sized contiguous colonies/spheroids. In addition, cells in PVA/Gel/*P.emblica* cryogels were dose-dependently affected by *P. emblica* in terms of proliferation and distrubition. In contrast, cells in PVA/Gel grew in scattered colonies and in fewer numbers. Unlike control cells, which grew in a monolayer in polystyrene, adherence and infiltration of cells into the cryogel were observed and their 3D structure was clear (Figure 9a,b). Cells show different structural conformations from typical images of cells adhering to 2D surfaces when in contact with 3D scaffolds. [73]. Cells in PVA/Gel and PVA/Gel/*P.emblica* cryogels retained a tightly arranged cubic/spherical morphology. F-Actin/DAPI staining showed peripheral accumulation of strongly organized F-actin following cell contours (Figure 9c) [74]. In this paper, it was observed that loading *P. emblica* on cryogel effectively enhanced cell number and adhesion in spherical morphology. However, morphological studies should be confirmed molecularly and biochemically for known morphological differentiation markers such as involucrin, cytokeratin, keratin and vimentin [75,76]. According to C-AM/Eth-1 staining, the compounds used in the synthesis of PVA/Gel and PVA/Gel/*P.emblica* cryogels did not affect cell viability. It was observed as live (green) and dead (red) cells with cubic boundaries inside the scaffold (Figure 9d). Our microscopic imaging data confirmed the cell viability and proliferation data, demonstrating good compatibility of PVA/Gel/*P.emblica* cryogels to keep a high number of cells viable in healthy morphology. Our data showed that PVA/Gel/*P.emblica* cryogels are suitable for use in skin tissue engineering applications and can be developed with advanced studies.

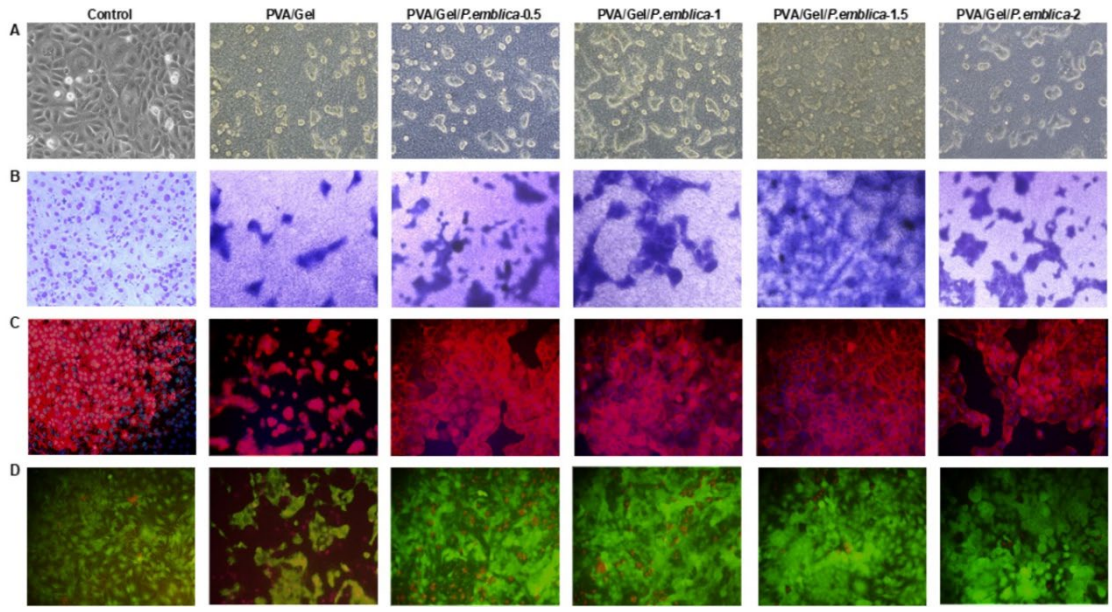

Figure 9. The effect of PVA/Gel and PVA/Gel/*P.emblica* cryogels on cells morphology, adhesion, viability cell-cell and cell-matrix interactions. Cell morphology was analyzed at 72 hour. The cells cultivated in polystyrene-culture plate were utilized as a control. Representative **(A)** phase contrast microscopy, **(B)** giemsa staining (pink-purple), **(C)** immunofluorescence of F-Actin (red)/ DAPI (blue) staining merge and **(D)** C-AM (green)/Eth-1 (red) staining images of seeded cells on control, PVA/Gel, PVA/Gel/*P.emblica*-0.5, PVA/Gel/*P.emblica*-1, PVA/Gel/*P.emblica*-1.5 and PVA/Gel/*P.emblica*-2 cryogels (all magnifications X20, scale bar: 100 μm). DAPI: 4′,6-diamidino-2-phenylindole; C-AM: Calcein

 doi:10.20944/preprints202311.1288.v2

Acetomethoxy; Eth-1: Ethidium homodimer-1; PVA/Gel: Poly (vinyl alcohol)/Gelatin cryogels; PVA/Gel/*P.emblica*: *P. emblica* loaded PVA/Gel cryogels; *P. emblica*: *Phyllanthus emblica*.

In a skin injury, migration and proliferation of keratinocytes are triggered first due to the inflammatory response, then they interact with the ECM and their adhesion changes [77]. Activation of keratinocyte migration is closely related to intercellular transmission and signal transduction regulated by Connexins, (Cx) proteins, which form an intercellular space junction [78]. In particular, gap junction protein Cx43 is involved in inducing signaling pathways including growth factors and ECM deposition that are key in wound closure [79]. Cx43 distribution in cells cultured on control, PVA/Gel, PVA/Gel/*P.emblica*-0.5, PVA/Gel/*P.emblica*-1, PVA/Gel/*P.emblica*-1.5 and PVA/Gel/*P.emblica*-2 cryogels was visualized under the microscope at 72nd h by immunofluorescence staining (Figure 10). Cx43 emits intense and bright fluorescent light in direct proportion to the increase in cell-cell interaction [71]. An overall increase in gap junction density was observed for cells cultured on PVA/Gel/*P.emblica* cryogels compared to control and PVA/Gel (Figure 10a–c). According to the quantitative analysis of immunofluorescent staining, Cx43 antibody fluorescence intensity in PVA/Gel/*P.emblica*-0.5, PVA/Gel/*P.emblica*-1, PVA/Gel/*P.emblica*-1.5 and PVA/Gel/*P.emblica*-2 cryogels was increased by 38.41% ± 8.02%, 131.03% ± 7.80%, 186.87% ± 10.62%, 311.93% ± 14.42% and 63.21% ± 8.35%, respectively, compared to control ($P < 0.0001$ for all). Moreover, gap junction density increased by 275.12%, 365.77%, 568.84% and 165.51% in PVA/Gel/*P.emblica*-0.5, PVA/Gel/*P.emblica*-1, PVA/Gel/*P.emblica*-1.5 and PVA/Gel/*P.emblica*-2 compared to PVA/Gel cryogel ($P < 0.0001$ for all). In addition, the fluorescence intensity of Cx43 increased by 56.09%, 69.64% and 39.70% in PVA/Gel/P.emblica-1.5 compared to other PVA/Gel/*P.emblica* cryogels, respectively (Figure 10d) ($P < 0.0001$ for all). This data generally indicates enhanced cell-to-cell interaction in cryogels loaded with *P. emblica* ($P = 0.0007$ for *P.emblica*-0.5/*P.emblica*-1; $P < 0.0001$ for *P.emblica*-0.5/*P.emblica*-2 and $P < 0.0001$ for *P.emblica*-1/*P.emblica*-2).

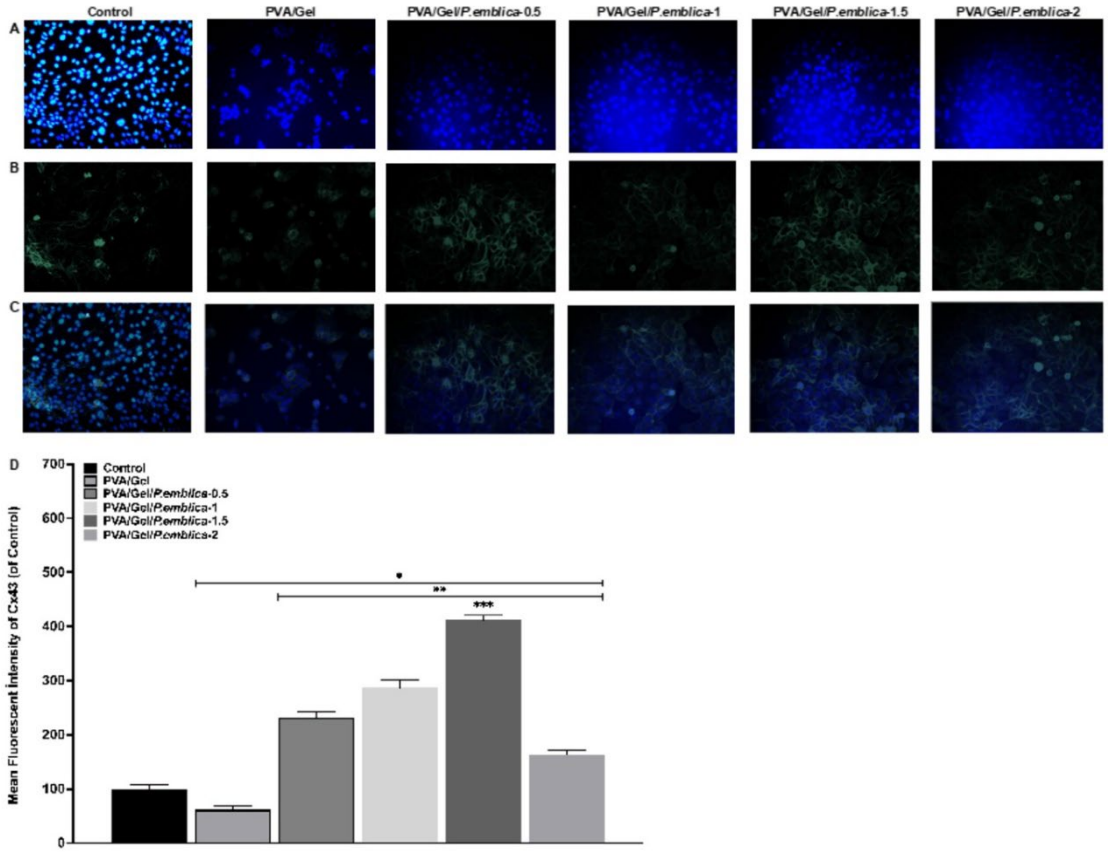

Figure 10. The effect of PVA/Gel and PVA/Gel/*P.emblica* cryogels on Cx43 distribution in cells by immunofluorescence staining. Cx43 staining was performed 72nd h after incubation. The cells

 doi:10.20944/preprints202311.1288.v2

cultivated in polystyrene-culture plate were utilized as a control. Representative **(A)** DAPI (blue), **(B)** Cx43 (green) and **(C)** immunofluorescence of Cx43 (green)/ DAPI (blue) staining merge images of seeded cells on control, PVA/Gel, PVA/Gel/*P.emblica*-0.5, PVA/Gel/*P.emblica*-1, PVA/Gel/*P.emblica*-1.5 and PVA/Gel/*P.emblica*-2 cryogels (all magnifications X20, scale bar: 100 μm). (**D)** Quantitative data of relative intensity of anti-Cx43 immunofluorescent staining. Six individual regions that randomly selected were imaged on each sample and the relative of fluorescent dye was measured using ImageJ software. Data were defined as relative variation of fluorescent signal intensities and mean ± SD (n= 3). One-way ANOVA test was used for statistical analysis. *P< 0.001 differ significantly from control. **P< 0.001 is significantly different from the PVA/Gel. ***P< 0.001 is significantly different from the PVA/Gel/*P.emblica*-1.5. DAPI: 4',6-diamidino-2-phenylindole; Cx43: Connexin 43; PVA/Gel: Poly (vinyl alcohol)/Gelatin cryogels; PVA/Gel/*P.emblica*: *P. emblica* loaded PVA/Gel cryogel; *P. emblica*: *Phyllanthus emblica*.

The purpose of biomaterial production is to form good cellular adhesion areas for controlling cell migration, proliferation, differentiation and ECM synthesis [80]. Cells were visualized 72 h after incubation to evaluate the effect of control, PVA/Gel, PVA/Gel/*P.emblica* cryogels on cell proliferation, morphology, localization and cell-matrix interaction by SEM. SEM can visualize cell attachment, spread, and morphology within the porous structure of the cryogel, revealing important information about the distribution of cells and their interaction with the surrounding matrix [81]. Cells with indistinct borders located in the pores of the scaffold and inside the polymeric walls grew on the cryogels and the presence of ECM was observed. There was also strong contact between cells and formed colonies/spheroids. It was observed that cells also encompass the interpore spaces, as evidenced by the spherical morphology covering the surface [74]. Notably, in the PVA/Gel/*P.emblica* cryogel compared to PVA/Gel, cells settled over the entire surface of the scaffold, forming diffuse, proliferating and contiguous colonies/spheroids with ECM formation. Cell number and density were affected by the *P. emblica* concentration in the cryogels (Figure 11). *P. emblica* contains bioactive secondary metabolites such as gallic acid, ascorbic ecid, quercetin, punigluconin, apigenin 7-glucoside, kaempferol and so on [29]. *P. emblica* loaded cryogels possess bioactive components with multiple hydroxyl functional groups that promote cell attachment as well as cell proliferation. Macroporosity in biomaterials allows nutrient supply and metabolic waste diffusion for cell-cell network formation [82]. The ECM is vital for cell adhesion, receiving-transmitting physical external stimuli, and has a significant impact on cellular behavior [70]. SEM data revealed that the macroporous structure of PVA/Gel/*P.emblica* cryogels promotes cell adhesion and growth to simulate epithelialization by synthesizing proinflammatory and growth factors from keratinocytes for wound healing [83]. In vitro results showed that the PVA/Gel/*P.emblica* cryogel, which provides versatile support for cell-material interaction with its 3D structure, has the potential to pave the way for the design of more efficient next generation tissue engineering materials and implants.

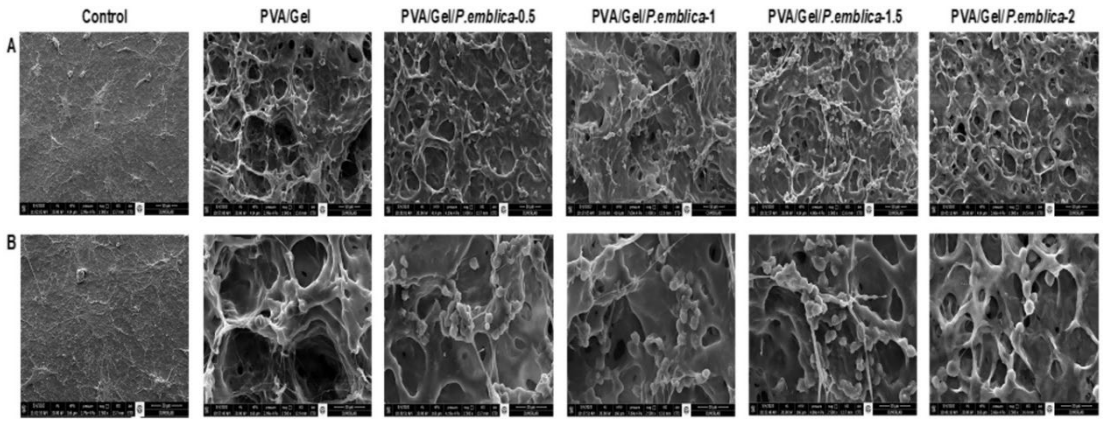

Figure 11. SEM images of PVA/Gel and PVA/Gel/*P.emblica* cryogels with cells. The cells cultivated in polystyrene-culture plate were utilized as a control. SEM images of seeded cells on control, PVA/Gel, PVA/Gel/*P.emblica*-0.5, PVA/Gel/*P.emblica*-1, PVA/Gel/*P.emblica*-1.5 and PVA/Gel/*P.emblica*-2 cryogels

 doi:10.20944/preprints202311.1288.v2

(**A)** at 1000X magnification, scale bar: 50 µm and **(B)** at magnification 2500X, scale bar: 30 µm. SEM: Scanning electron microscopy; PVA/Gel: Poly (vinyl alcohol)/Gelatin cryogels; PVA/Gel/*P.emblica*: *P. emblica* loaded PVA/Gel cryogels; *P. emblica*: *Phyllanthus emblica*.

3.7. Cell adhesion and Infiltration on PVA/Gel and PVA/Gel/P.emblica Cryogels by DAPI and F-Actin Staining

In tissue engineering applications, the suitability of the biomaterial is important for cells to attach, infiltrate, multiply, grow and differentiate [52]. Cell nuclei and cytoplasm were stained with DAPI and phalloidin to test cell adhesion and infiltraion matrix cultured on PVA/Gel, PVA/Gel/*P.emblica*-0.5, PVA/Gel/*P.emblica*-1, PVA/Gel/*P.emblica*-1.5 and PVA/Gel/*P.emblica*-2 cryogels at 72 h [83]. (Figure 12). Thanks to the porous structure of the cryogels, homogeneous cells that adhered to the matrices were visualized under a fluorescent microscope by staining with DAPI and F-Actin. A strong fluorescence was observed showing a highly populated, matrix-penetrating cells evenly dispersed within the pores of the PVA/Gel/*P.emblica* cryogels compared to the control and PVA/Gel. The interconnected pores forming the structure of the cryogel allowed the cells to settle. In contrast, an opaque and weakly fluorescence was observed in PVA/Gel, indicating a limited number of diffuse, clustered, and few cells on the surface. PVA and gelatin scaffolds are widely used for tissue engineering applications with their biocompatible nature [56]. It has been reported that vascularization, epithelialization, cell proliferation, adhesion and migration can be stimulated by loading different bioactive compounds into the PVA/Gel cryogel [43,59]. It is known that *P. emblica* is rich in phytochemicals, has high free radical scavenging and antioxidant activity, as well as wound healing ability by inducing cell attachment, proliferation and migration in many cell types [28,29,85]. The release of biomolecules in the *P. emblica* extract into the matrix was not specifically investigated in this study. However, considering the literature, it is thought that the molecules in the *P. emblica* remain active even after *P. emblica* added into PVA/Gel cryogel, thus ultimately increasing the bioactivity of the material and promoting cell attachment and penetration [29,69,86].

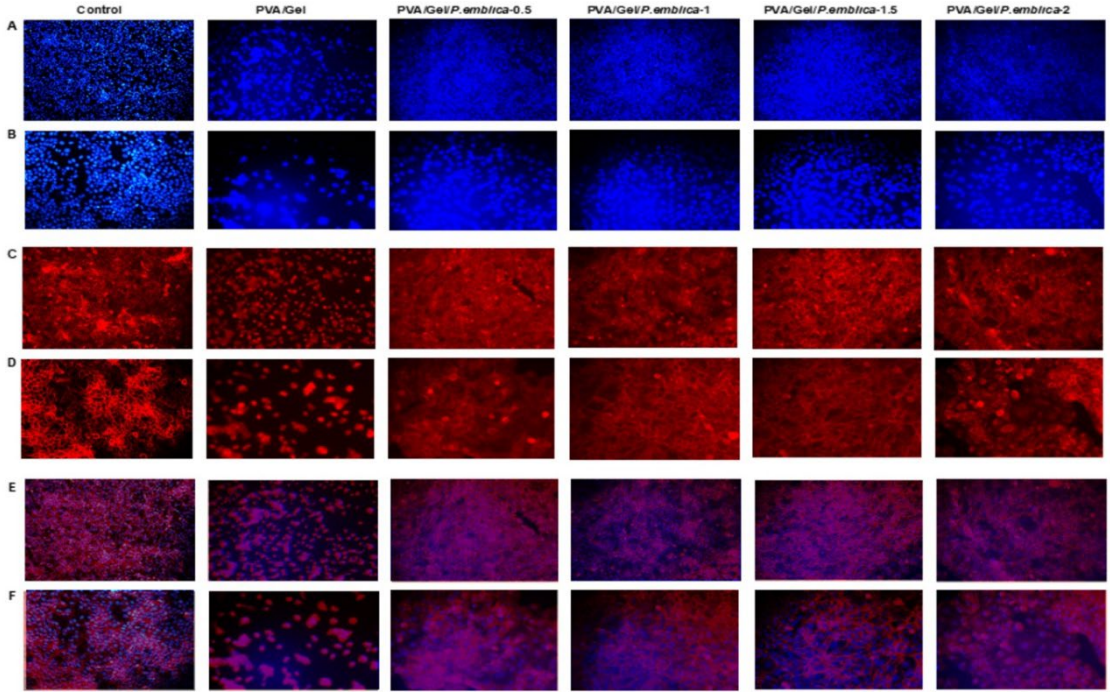

Figure 12. The effect of PVA/Gel and PVA/Gel/*P.emblica* cryogels on interaction of cells matrix via DAPI and F-actin staining. The cells cultivated in polystyrene-culture plate were utilized as a control. Representative **(A), (B)** DAPI and **(C), (D)** F-Actin and **(E) (F)** DAPI/F-Actin staining merge images of cells in control, PVA/Gel, PVA/Gel/*P.emblica*-0.5, PVA/Gel/*P.emblica*-1, PVA/Gel/*P.emblica*-1.5 and PVA/Gel/*P.emblica*-2 cryogels. Top row images at 10X magnification, scale bar: 150 µm and bottom row images at magnification 20X, scale bar: 100 µm. DAPI: 4',6-diamidino-2-phenylindole; PVA/Gel:

 doi:10.20944/preprints202311.1288.v2

Poly (vinyl alcohol)/Gelatin cryogels; PVA/Gel/*P.emblica*: *P. emblica* loaded PVA/Gel cryogels; *P. emblica*: *Phyllanthus emblica*.

4. Conclusion

In this study, *P. emblica*, a natural compound known to have antioxidant, anti-inflammatory and antimicrobial properties, was synthesized by adding into PVA/Gel cryogels. This study provides valuable insights into the development and characterization of cryogels loaded with *P. emblica* extract for potential use as wound dressings. *P. emblica* has a strong effect on accelerating wound healing, therefore PVA/Gel/*P.emblica* cryogels offered better cell viability and proliferation rate than PVA/Gel cryogels. Macroporous PVA-Gel/*P.emblica* cryogel was found to be non-cytotoxıc and biocompatible. The PVA/Gel/*P.emblica*-1.5 cryogel showed promising results with the highest swelling rate, cell viability and cell infiltration. Overall, it has been observed that *P. emblica* loaded cryogels have the potential to be used as wound dressings and scaffolds in tissue engineering applications. The study was based on in vitro analysis. Therefore, further studies and evaluations including in vivo studies can be needed to confirm and optimize the PVA/Gel/*P.emblica* cryogels for specific wound dressing applications and to understand the release profile of bioactive compounds from *P. emblica* within the cryogel.

Author Contributions: Conceptualization, İ.C. and S.Ö.; methodology, S.Ö., İ.C. and G.B.P.; software, İ.C and S.Ö.; validation, S.Ö. and G.B.P.; formal analysis, İ.C. and S.Ö.; investigation, İ.C., S.Ö. and G.B.P.; resources, İ.C., S.Ö. and G.B.P.; data curation, İ.C., S.Ö. and G.B.P.; writing—original draft preparation, İ, C.; writing—review and editing, İ.C., S.Ö. and G.B.P.; visualization, İ.C. and S.Ö.; supervision, S.Ö. and G.B.P.; project administration, İ.C and S.Ö.; funding acquisition, İ.C and S.Ö. All authors have read and agreed to the published version of the manuscript.

Funding: This work was supported by the ATU BAP Coordination Unit under Grant [number 22303016].

Conflict of Interest: The authors declare that they have no conflict of interest.

References

1. Farley A, McLafferty E, Hendry C. Cells, tissues, organs and systems. Nurs Sand. 2012;26(52):40. doi: 10.7748/ns2012.08.26.52.40.c9248
2. Dai T, Kharkwal GB, Tanaka, M, et al. Animal models of external traumatic wound infections. Virulence. 2011;*2*(4):296-315. doi: 10.4161/viru.2.4.16840
3. Gobi R, Ravichandiran P, Babu R, et al. Biopolymer and synthetic polymer-based nanocomposites in wound dressing applications: a review. Polymers. 2021;13(12):1962. doi: 10.3390/polym13121962
4. Koyutürk A, Soyaslan D. Yara ve yanık tedavisinde kullanılan örtüler. MAKÜ FEBED. 2016;*7*(Special Issue 1): p. 58-65.
5. Dabiri G, Damstetter E, Phillips T. Choosing a wound dressing based on common wound characteristics. Adv Wound Care. 2016;*5*(1): 32-41. doi: 10.1089/wound.2014.0586.
6. Han G, Ceilley R. Chronic wound healing: a review of current management and treatments. Adv Ther. 2017;*34*(3):599-610. doi: 10.1007/s12325-017-0478-y
7. Schoukens G. Advanced Textiles for Wound Care. 2nd ed. Cambridge: Woodhead Publishing; 2019. Bioactive dressings to promote wound healing; p. 135–167. doi: 10.1533/9781845696306.1.114
8. Liang Y, He J, Guo B. Functional hydrogels as wound dressing to enhance wound healing. *ACS Nano*. 2021;*15*(8):12687-12722. doi: 10.1021/acsnano.1c04206
9. Kamoun E. A, Kenawy E. R. S, Chen X. A review on polymeric hydrogel membranes for wound dressing applications: PVA-based hydrogel dressings. J Adv Res. 2017;*8*(3):217-233. doi: 10.1016/j.jare.
10. Akin B, Ozmen M. M. Antimicrobial cryogel dressings towards effective wound healing. *Prog Biomater*. 2022:1-16. doi: 10.1007/s40204-022-00202-w
11. Tripathi A, Vishnoi T, Singh D, et al. Modulated crosslinking of macroporous polymeric cryogel affects in vitro cell adhesion and growth. Macromol Biosci. 2013;*13*(7): 838-850. doi: 10.1002/mabi.201200398
12. Shirbin S. J, Lam S. J, Chan N. J. A, Ozmen M. M, et al. Polypeptide-based macroporous cryogels with inherent antimicrobial properties: the importance of a macroporous structure. *ACS Macro Lett*. 2016:*5*(5); 552-557. doi: 10.1021/acsmacrolett.6b00174
13. Memic A, Colombani T, Eggermont L. J, et al. Latest advances in cryogel technology for biomedical applications. Adv Ther. 2019;*2*(4):1800114. doi: 10.1002/adtp.201800114

14. Eigel D, Werner C, Newland B. Cryogel biomaterials for neuroscience applications. Neurochem Int. 2021;(*147*):105012. doi: 10.1016/j.neuint.2021.105012
15. Moura L. I, Dias A. M, Carvalho E, et al. (2013). Recent advances on the development of wound dressings for diabetic foot ulcer treatment—A review. Acta Biomater. 2013;*9*(7):7093-7114. doi: 10.1016/j.actbio.2013.03.033
16. Vishnoi, T. In *3D Printing in Medicine and Surgery*. Cambridge: Woodhead Publishing; 2021. 3D bioprinting of tissue systems; p. 171-197.
17. Singh S, Gaikwad K. K, Lee Y. S. Antimicrobial and antioxidant properties of polyvinyl alcohol bio composite films containing seaweed extracted cellulose nano-crystal and basil leaves extract. Int J Biol Macromol. 2018;*107*:1879-1887. doi: 10.1016/j.ijbiomac.2017.10.057
18. Liu X, Jia G. Modern wound dressing using polymers/biopolymers. J Material Sci Eng. 2018;7(3). doi: 10.4172/2169-0022.1000454
19. Maver T, Maver U, Kleinschek K. S, et al. A review of herbal medicines in wound healing. Int J Dermatol. 2015;54(7):740-751. doi: 10.1111/ijd.12766
20. Gaspar-Pintiliescu A, Stanciuc A. M, Craciunescu O. Natural composite dressings based on collagen, gelatin and plant bioactive compounds for wound healing: A review. Int J Biol Macromol .2019;(*138)*: 854-865. doi: 10.1016/j.ijbiomac.2019.07.155
21. Rezvani Ghomi E, Khalili S, Nouri Khorasani S, (2019). Wound dressings: Current advances and future directions. *J Appl Polym Sci*. 2019;*136*(27):47738. doi: https://doi.org/10.1002/app.47738
22. Joseph N, Rao MPB, Geevarughese NM, et al. *Bioactive Dietary Factors and Plant Extracts in Dermatology*. Humana Press: Totowa; *2013*. Amla (Emblica officinalis Gaertn.) the Indian indigenous berry in skin care. p. 113-123. doi: 10.1007/978-1-62703-167-7_12
23. Khan K. H. Roles of Emblica officinalis in medicine-A review. Bot Res Int. 2009; 2(4): 218-228. doi: 1995-8951
24. Jayaweera DMA. Medicinal plants (Indigenous and exotic) used in Ceylon. Colombo: National Science Council of Sri Lanka; 1980.
25. Bhandari P. R, Kamdod M. A. Emblica officinalis (Amla): A review of potential therapeutic applications. Int J Green Pharm. 2012:*6*(4);257. doi: 10.4103/0973-8258.108204
26. Kulkarni K. V, Ghurghure S. M. Indian gooseberry (Emblica officinalis): Complete pharmacognosy review. *Int J Chem Stud*. 2018; 2(2):5-11. doi: 2581-348X
27. Khan M. S, Qais F. A, Ahmad I. New Look to Phytomedicine: Advancements in Herbal Products as Novel Drug Leads. Amsterdam (Netharlands): Elsevier Academic Press; 2019. Indian berries and their active compounds: Therapeutic potential in cancer prevention; p. 179-201. doi: 10.1016/B978-0-12-814619-4.00008-2
28. Talekar Y. P, Apte K. G, Paygude S. V, et al. Studies on wound healing potential of polyherbal formulation using in vitro and in vivo assays. J Ayurveda Integr Med. 2017;*8*(2):73-81. doi: 10.1016/j.jaim.2016.11.007
29. Ahmad B, Hafeez N, Rauf A, et al. Phyllanthus emblica: A comprehensive review of its therapeutic benefits. S Afr J Bot. 2021;*138*: 278-310. doi: https://doi.org/10.1016/j.sajb.2020.12.028
30. Chularojmontri L, Suwatronnakorn M, Wattanapitayakul S. K. Phyllanthus emblica L. enhances human umbilical vein endothelial wound healing and sprouting. Evid Based Complement Alternat Med. 2013;2013:720728. doi: 10.1155/2013/720728.
31. Klimis-Zacas D, Rodriguez-Mateos A. Berries and Berry Bioactive Compounds in Promoting Health. United Kingdom: Royal Society of Chemistry; 2022.
32. Perçin I, Idil N, Denizli A. Molecularly imprinted poly (N-isopropylacrylamide) thermosensitive based cryogel for immunoglobulin G purification. Process Biochemistry. 2019;80, 181-189. doi: 10.1016/j.procbio.2019.02.001
33. Fan M, Gong L, Huang Y, Wang D, Gong Z. Facile preparation of silver nanoparticle decorated chitosan cryogels for point-of-use water disinfection. Science of the Total Environment. 2018;613, 1317-1323. doi: 10.1016/j.scitotenv.2017.09.256
34. Gun'ko V. M, Savina I. N, Mikhalovsky S. V. Cryogels: Morphological, structural and adsorption characterisation. Adv Colloid Interface Sci.2013;*187*:1-46. doi: 10.1016/j.cis.2012.11.001.
35. Górska A, Krupa A, Majda D, et al. Poly (Vinyl alcohol) cryogel membranes loaded with resveratrol as potential active wound dressings. AAPS PharmSciTech. 2021; 22:1-14. doi: 10.1208/s12249-021-01976-1
36. Xu N, Yuan Y, Ding L, et al. Multifunctional chitosan/gelatin@ tannic acid cryogels decorated with in situ reduced silver nanoparticles for wound healing. Burns Trauma. 2022;*10*. doi: 10.1093/burnst/tkac019
37. Nikhil A, Kumar A. Evaluating potential of tissue-engineered cryogels and chondrocyte derived exosomes in articular cartilage repair. Biotechnol Bioeng. 2022;*119*(2):605-625. doi: 10.1002/bit.27982
38. Hobro A. J, Smith N. I. An evaluation of fixation methods: Spatial and compositional cellular changes observed by Raman imaging. Vib Spectrosc. 2017;91:31-45. doi: 10.1016/j.vibspec.2016.10.012

39. Zhang T, Wang Y, Xia Q, et al. Propofol mediated protection of the brain from ischemia/reperfusion injury through the regulation of microglial connexin 43. Front Cell Dev Biol. 2021;*9*:637233. doi: 10.3389/fcell.2021.637233
40. Gülnar B, Canatar İ, Özdaş S. Antiadipogenic and antiobesogenic effects of pterostilbene in 3T3-L1 preadipocyte models. *Turk J Biol*. 2023;*47*(2): 130-140. doi: 10.55730/1300-0152.2649
41. Gugliuzza A. Encyclopedia of Membranes. Berlin, Heidelberg: Springer; 2016. Solvent Swollen Polymer; p. 1801–1802. doi: 10.1007/978-3-662-44324-8_1407
42. Shetty G. R, Rao B. L. Preparation and characterization of silk fibroin-polyvinyl alcohol (PVA) blend films for food packaging materials. Materials Today: Proceedings. 2022;55:194-200. doi: 10.1016/j.matpr.2022.02.034
43. Choi S. M, Singh D, Kumar A, et al. Porous three-dimensional PVA/gelatin sponge for skin tissue engineering. Int J Polym Mater Polym Biomater.2013;62(7):384-389. doi: 10.1080/00914037.2012.710862
44. Jones LO, Williams L, Boam T, et al. Cryogels: recent applications in 3D-bioprinting, injectable cryogels, drug delivery, and wound healing. Beilstein J Org Chem. 2021;17(1): 2553-2569. doi: 10.3762/bjoc.17.171
45. Derazshamshir A, Baydemir G, Andac M, et al. Molecularly imprinted PHEMA-based cryogel for depletion of hemoglobin from human blood. *Macromol Chem Phy*. 2010;*211*(6):657-668. doi: 10.1002/macp.200900425
46. Huang M. R, Li X. G, Yang Y. Oxidative polymerization of o-phenylenediamine and pyrimidylamine. Polym Degrad Stab. 2000;*71*(1): 31-38. doi: 10.1016/S0141-3910(00)00137-3
47. Du Toit J. P, Pott R. W. Transparent polyvinyl-alcohol cryogel as immobilisation matrix for continuous biohydrogen production by phototrophic bacteria. Biotechnol Biofuels. 2020;13(1): 1-16. doi: 10.1186/s13068-020-01743-7
48. Liu Y, Vrana N.E, Cahill P.A, et al. Physically crosslinked composite hydrogels of PVA with natural macromolecules: Structure, mechanical properties, and endothelial cell compatibility. J Biomed Mater Res B Appl Biomater. 2009;90: 492-502. doi: 10.1002/jbm.b.31310
49. Razavi M, Qiao Y, Thakor A. S. Three-dimensional cryogels for biomedical applications. J Biomed Mater Res A. 2019;107(12): 2736-2755. doi: 10.1002/jbm.a.36777
50. Teixeira, V. S., Kalckhoff, J. P., Krautschneider, W., Schroeder, D. Bioimpedance analysis of L929 and HaCaT cells in low frequency range. Current directions in biomedical engineering. 2018; 4(1): 115-118.
51. Shakya A. K, Holmdahl R, Nandakumar K. S, et al. Polymeric cryogels are biocompatible, and their biodegradation is independent of oxidative radicals. J Biomed Mater Res A. 2014;102(10):3409-3418. doi: 10.1002/jbm.a.35013
52. Kathuria N, Tripathi A, Kar K. K, et al. Synthesis and characterization of elastic and macroporous chitosan–gelatin cryogels for tissue engineering. Acta Biomater. 2009;5(1):406-418. doi: 10.1016/j.actbio.2008.07.009
53. Kao H. H, Kuo C. Y, Chen K. S, et al. . Preparation of gelatin and gelatin/hyaluronic acid cryogel scaffolds for the 3D culture of mesothelial cells and mesothelium tissue regeneration. Int J Mol Sci. 2019;*20*(18): 4527. doi: 10.3390/ijms20184527
54. Muppalaneni S, Omidian H. Polyvinyl alcohol in medicine and pharmacy: a perspective. *J. Dev. Drugs*. 2013;*2*(3):1-5. doi: 10.4172/2329-6631.1000112
55. Farris S, Song J, Huang Q. Alternative reaction mechanism for the cross-linking of gelatin with glutaraldehyde. J Agric Food Chem. 2010;*58*(2):998-1003. doi:
56. He Y, Wang C, Wang C, et al. An overview on collagen and gelatin-based cryogels: fabrication, classification, properties and biomedical applications. Polymers, 2021;13(14): 2299. doi: 10.3390/polym13142299
57. Charron P. N, Jacobs J. I, Yao S. X, et al. Effects of cryo-processing on the mechanical and biological properties of poly (vinyl alcohol)-gelatin theta-gels. Biointerphases. 2020;15(5). doi: 10.1116/6.0000381
58. Cheaburu-Yilmaz C. N, Yilmaz O, Aydin Kose F, et al. Chitosan-graft-poly (N-isopropylacrylamide)/PVA cryogels as carriers for mucosal delivery of voriconazole. *Polymers*. 2019;*11*(9):1432. doi: 10.3390/polym11091432
59. Vrana N. E, Cahill P. A, McGuinness G. B. Endothelialization of PVA/gelatin cryogels for vascular tissue engineering: Effect of disturbed shear stress conditions. J Biomed Mater Res *A*. 2010;*94*(4):1080-1090. doi: 10.1002/jbm.a.32790
60. Liao T. T, Sukpat S, Chansriniyom C, et al. Topical combined Phyllanthus emblica Linn. and simvastatin improves wound healing in diabetic mice by enhancing angiogenesis and reducing neutrophil infiltration. Biomed Rep. 2023;18(4): 1-11. doi: 10.3892/br.2023.1613
61. Suvandee W, Teeranachaideekul V, Jeenduang N, et al. One-Pot and Green Preparation of Phyllanthus emblica Extract/Silver Nanoparticles/Polyvinylpyrrolidone Spray-On Dressing. Polymers. 2022;14(11):2205. doi: 10.3390/polym14112205
62. Lin Y. Y, Lu S. H, Gao R, et al. A novel biocompatible herbal extract-loaded hydrogel for acne treatment and repair. Oxid Med and Cell Longev. 2021;2021. doi: 10.1155/2021/5598291

63. Abd El-Aziz A. M, El-Maghraby A, Ewald A, et al. In-vitro cytotoxicity study: cell viability and cell morphology of carbon nanofibrous scaffold/hydroxyapatite nanocomposites. Molecules. 2021;26(6):1552. doi: 10.3390/molecules26061552
64. Pavez Lorie E, Stricker N, Plitta-Michalak B, et al. Characterisation of the novel spontaneously immortalized and invasively growing human skin keratinocyte line HaSKpw. Sci Rep. 2020;10(1):15196. doi: 10.1038/s41598-020-71315-0
65. Pessina A, Raimondi A, Cerri A, et al. High sensitivity of human epidermal keratinocytes (HaCaT) to topoisomerase inhibitors. Cell Prolif. 2021;34(4):243-252. doi: 10.1046/j.0960-7722.2001.00214.x
66. Stoker M. G. P, Rubin H. Density dependent inhibition of cell growth in culture. Nature.1967;215(5097):171-172. doi: 10.1038/215171a0
67. Guo B, Dong R, Liang Y, et al. Haemostatic materials for wound healing applications. Nat Rev Chem. 2021;5(11):773-791. doi: 10.1038/s41570-021-00323-z
68. Lemos N. E, Brondani L. D. A, Dieter C, et al. Use of additives, scaffolds and extracellular matrix components for improvement of human pancreatic islet outcomes in vitro: A systematic review. Islets. 2017;9(5):73-86. doi: 10.1080/19382014.2017.1335842
69. Liu M, Dai Y, Li Y, et al. Madecassoside isolated from Centella asiatica herbs facilitates burn wound healing in mice. Planta Med. 2008;74(08):809-815. doi: 10.1055/s-2008-1074533
70. Boudreau N. J, Jones P. L. Extracellular matrix and integrin signalling: the shape of things to come. Biochem J. 1999;*339*(3):481-488. doi: 10215583
71. Entcheva E, Bien H, Yin L, et al. Functional cardiac cell constructs on cellulose-based scaffolding. *Biomaterials*.2004;*25*(26):5753-5762.doi: 10.1016/j.biomaterials.2004.01.024
72. Ma Y, Wang X, Su T, et al. Recent advances in macroporous hydrogels for cell behavior and tissue engineering. *Gels*. 2022;*8*(10):606. doi: 10.3390/gels8100606
73. Eyckmans J, Chen C. S. 3D culture models of tissues under tension. J Cell Sci. 2017;*130*(1): 63-70. doi: 10.1242/jcs.198630
74. Boukamp P, Petrussevska R. T, Breitkreutz D, et al. Normal keratinization in a spontaneously immortalized aneuploid human keratinocyte cell line. J Cell Biol. 1988;106(3):761-771. doi: 10.1083/jcb.106.3.761
75. Borowiec A. S, Delcourt P, Dewailly E, et al. Optimal differentiation of in vitro keratinocytes requires multifactorial external control. *PloS one*. 2013;*8*(10):e77507. doi: 10.1371/journal.pone.0077507
76. Breitkreutz D, Stark H. J, Plein P, et al. Differential modulation of epidermal keratinization in immortalized (HaCaT) and tumorigenic human skin keratinocytes (HaCaT-ras) by retinoic acid and extracellular Ca2+. *Differentiation*. 1993;*54*(3):201-217. doi: 10.1111/j.1432-0436.1993.tb01602.x
77. Stojadinovic O, Brem H, Vouthounis C, et al. Molecular pathogenesis of chronic wounds: the role of β-catenin and c-myc in the inhibition of epithelialization and wound healing. Am J Pathol. 2005;167(1):59-69. doi: 10.1016/s0002-9440(10)62953-7
78. Langlois S, Maher A. C, Manias J. L, et al. Connexin levels regulate keratinocyte differentiation in the epidermis. J Biol Chem. 2007;282(41):30171-30180. doi: 10.1074/jbc.M703623200
79. Faniku C, O'Shaughnessy E, Lorraine C, et al. The connexin mimetic peptide Gap27 and Cx43-knockdown reveal differential roles for Connexin43 in wound closure events in skin model systems. Int J Mol Sci. 2018;19(2):604. doi: 10.3390/ijms19020604
80. Langer R, Tirrell D. A. Designing materials for biology and medicine. Nature. 2004;428(6982):487-492. doi: 10.1038/nature02388
81. Iandolo D, Pennacchio F. A, Mollo V, et al. Electron microscopy for 3D scaffolds–cell biointerface characterization. Adv Biosyst. 2019;3(2):1800103. doi: 10.1002/adbi.201800103
82. Deb P, Deoghare A. B, Borah A, et al. Scaffold development using biomaterials: a review. Mater Today Proc. 2018;5(5):12909-12919. doi: 10.1016/j.matpr.2018.02.276
83. Werner S, Krieg T, Smola H. Keratinocyte–fibroblast interactions in wound healing. J Invest Dermatol. 2007;127(5):998-1008. doi: 10.1038/sj.jid.5700786
84. Afanasiev SA, Muslimova EF, Nashchekina YA et al. Peculiarities of Cell Seeding on Electroformed Polycaprolactone Scaffolds Modified with Surface-Active Agents Triton X-100 and Polyvinylpyrrolidone. *Bull Exp Biol Med. 2020;169*:600-604. doi: 10.1007/s10517-020-04936-0
85. Datta H. S, Mitra S. K, Patwardhan B. Wound healing activity of topical application forms based on ayurveda. Evid Based Complement Alternat Med. 2011;*2011*:134378. doi: 10.1093/ecam/nep015
86. Hixon K. R, Lu T, Sell S. A. A comprehensive review of cryogels and their roles in tissue engineering applications. *Acta Biomater.* 2017;*62*:29-41. doi: 10.1016/j.actbio.2017.08.033